FE-2030-7

THE CHARACTERISTICS OF AMERICAN COALS IN RELATION TO THEIR CONVERSION INTO CLEAN ENERGY FUELS

Quarterly Technical Progress Report, January—March 1977

By
W. Spackman
A. Davis
P. L. Walker
H. L. Lovell
R. H. Essenhigh
F. J. Vastola
P. H. Given

June 1977
Date Published

Work Performed Under Contract No. EX-76-C-01-2030

Coal Research Section
The Pennsylvania State University
University Park, Pennsylvania

U. S. DEPARTMENT OF ENERGY

DISCLAIMER

NOTICE

FE-2030-7
Distribution Categories UC-90a, UC-90b, UC-90c, UC-90d, UC-90e

THE CHARACTERISTICS OF AMERICAN COALS IN RELATION TO THEIR CONVERSION INTO CLEAN ENERGY FUELS

Quarterly Technical Progress Report

January - March 1977

by
W. Spackman, A. Davis, P.L. Walker, H.L. Lovell,
R.H. Essenhigh, F.J. Vastola and P.H. Given

COAL RESEARCH SECTION
THE PENNSYLVANIA STATE UNIVERSITY
UNIVERSITY PARK, PENNSYLVANIA 16802

ABSTRACT

Under Facet I, 21 coal samples have been added to the Penn State/ERDA Coal Sample Bank. Ninety-six sets of analytical data and 114 coal samples were provided upon request to other agencies engaged in coal research.

Mass spectrometer and reactor systems (under Facet IV-A) have been used successfully in measuring the amount of vaporization (and pyrolysis) products of hydrocarbons in low concentrations in a helium carrier gas.

Facet IV-B research has shown, using small angle x-ray scattering, that the pore structure of a char is a function of the rank of the parent coal and maximum heat treatment temperature. Carbon deposition on chars from the cracking of methane decreases subsequent reactivity of the char to air. The decrease in reactivity appears to be due to a decrease in active surface area and deactivation of catalytic impurities.

Experimental results previously obtained concerning the combustion of char and anthracite (Facet V-A) have been analyzed with respect to a simple theory of radiative flame propagation and the computer model has been used to investigate the effects of fuel particle density variations.

In the study of the combustion characteristics of coal-oil-water emulsions (Facet V-B), furnace efficiency peaked at about 5 percent coal addition, at 10 percent water, and 20 percent excess air.

TABLE OF CONTENTS

	Page
ABSTRACT	ii
OBJECTIVE AND SCOPE OF WORK	iv
TASK DESCRIPTIONS	v
SUMMARY OF PROGRESS TO DATE	1
SAMPLE COLLECTION AND SEAM CHARACTERIZATION	4
Coal Sampling	4
COAL CHARACTERIZATION	5
Coal Characterization	5
Rapid Scan Automated Reflectance Microscope System	5
Hot-Stage Microscopy	7
SAMPLE BANK OPERATION, MAINTENANCE, AND DEVELOPMENT	8
Service to Other Agencies	8
PENN STATE/ERDA COAL DATA BASE	9
Coal Data Base Activity Report	9
REACTOR DEVELOPMENT AND OPERATION	11
Evaluation of the Gasification Potential of Coals	11
Effect of Heating Rate and Soak Temperature on Volatile Matter Release	13
Characteristics of Chars Produced by Pyrolysis Following Rapid Heating of Pulverized Coal	16
COKES AND CHARS	24
Methanol and Water Densities of Coal Chars	24
Small Angle X-ray Studies on Coal Chars	24
Effect of Carbon Deposition on the Porosity and Reactivity of Chars	26
Chemisorption of Oxygen on Carbonaceous Solids	30
Catalytic Activity of Minerals for the Cracking of Methane	36
COMBUSTION OF CHARS AND LOW VOLATILE FUELS	38
Combustion of Char and Anthracite Coal in Large Utility Boilers	38
COMBUSTION OF COAL-OIL EMULSIONS	48
Combustion of Coal-Oil-Water Mixture	48
CONCLUSIONS	52
REFERENCES	54
CONTRIBUTORS	56

OBJECTIVE AND SCOPE OF WORK

The primary objective of the overall program is to achieve the capability of predicting, from a knowledge of coal composition, the behavior of a coal in pre-conversion processing, coal gasification and coal liquefaction processes.

It is reasonable to ask if this goal is in fact attainable, recognizing the heterogeneity of coal seams. Clearly, it is not if one concerns oneself simply with the rank of the coal seam and its aggregate chemistry. A high volatile B coal from Indiana need not react to processing in the same manner as a high volatile B coal from Utah, even though their "chemistries" may be very similar. In contrast, a coal lithotype of a specific kind, at a given level of rank, can be expected to behave consistently, whether it derives from Alabama or Pennsylvania. Hence, the goal may very well be attainable if, as in the case of coal carbonization, we concern ourselves with the reacting entities and the properties of the important lithotypes.

The goal is to attain the same high level of predictive accuracy that is now found in the area of coal carbonization, where Penn State's collaborative work with the steel industry proved highly successful. To achieve this goal Penn State has devised an integrated program in which the success of the research is highly dependent on the effective operation of ALL of the program's Facets and Sub-facets which are as follows:

Facet I: Characterization of the Nation's Coal Resources
- I-A: Sample Collection and Seam Characterization
- I-B: Coal Characterization
- I-C: Sample Bank Operation, Maintenance and Development
- I-D: Penn State-ERDA Coal Data Base

Facet II: Coal Beneficiation and Pre-Use Processing

Facet IV: Significance of Coal Characteristics in Gasification Processes
- IV-A: Reactor Development and Operation
- IV-B: Cokes and Chars
- IV-D: Reactivity of Coal Chars
- IV-E: Catalysis Research
- IV-F: Differential Scanning Calorimetry

Facet V: Coal Combustion Research
- V-A: Combustion of Chars and Low Volatile Fuels
- V-B: Combustion of Coal-Oil Emulsions

THE CHARACTERISTICS OF AMERICAN COALS IN RELATION TO THEIR CONVERSION INTO CLEAN ENERGY FUELS

TASK DESCRIPTIONS

FACET I-A	Sample Collection and Seam Characterization
Task 1	Sampling Survey
Task 2	Sampling Plan
Task 3	Sampling
FACET I-B	Coal Characterization
Task 5	Characteristics and Use Potential of U. S. Coal Seams
Task 6	Characterization of Other ERDA Contractor Samples
Task 7	Automation of Microscopic Analytical Methods
FACET I-C	Sample Bank Operation, Maintenance and Development
Task 8	Maintenance of Coal Sample Bank
Tasks 9-14	Provision of Samples and Data to Penn State and Other Investigators
FACET I-D	Penn State/ERDA Coal Data Base
Task 15	Computerization of Data
Task 16	Evaluation of the Data Base
Task 17	Structuring and Utilization of the Data Base
FACET II	Coal Beneficiation and Pre-Use Processing
Task 18	Washability Characterization
Task 19	Physical Properties of Coal Lithotypes
Task 20	Techniques for Fractionation
Task 21	Beneficiation of Conversion Feedstocks
Task 22	Evaluation of Dry Flo Separator
FACET IV-A	Reactor Development and Operation
Task 23	Operation of Isothermal Furnace
Task 24	Pyrolysis of Coal Lithotypes
Task 25	Operation of Pressurized Isothermal Reactor
Task 26	Coal Reactivity
FACET IV-B	Cokes and Chars
Task 27	Effect of Variables on Char Structures
Task 28	Effect of Char Structures on Reactivities
Task 29	Catalytic Effect of Minerals in Gasification
Task 30	Effect of Catalytic Cations on Gasification
FACET IV-F	Differential Scanning Calorimetry
Task 31	DSC in Evaluating Coals for Conversion
FACET V-A	Combustion of Chars and Low Volatile Fuels
Task 32	Flame Ball Combustion Model
Task 33	Plane Flame Furnace
FACET V-B	Combustion of Coal - Oil Emulsions
Task 34	Combustion of Coal - Oil Emulsions

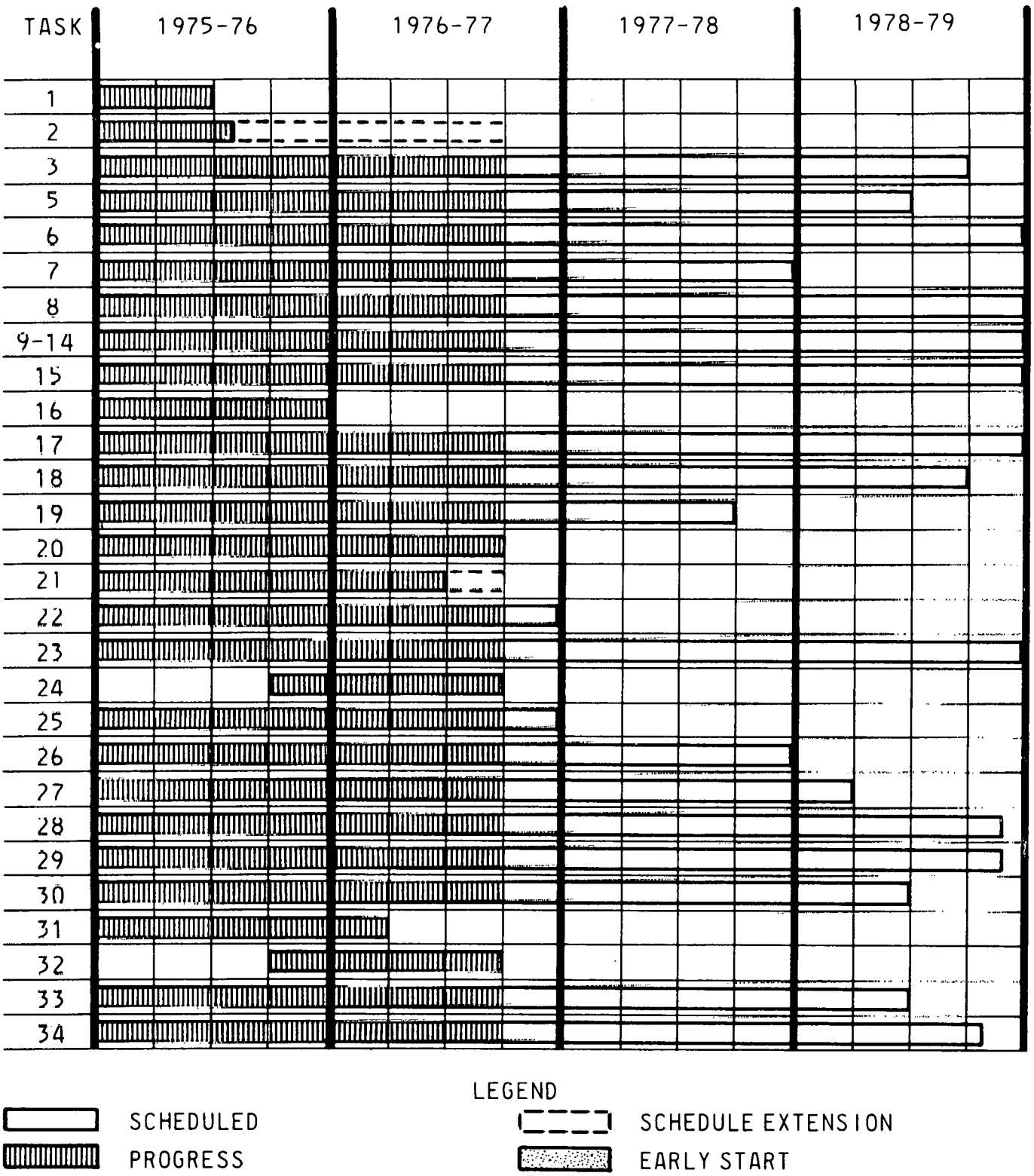

PROJECT PLAN AND PROGRESS REPORT

Quarter Ending March 31, 1977

SUMMARY OF PROGRESS TO DATE

Under Facet I the Penn State/ERDA Coal Sample Bank was enlarged to include 21 new coal samples. A total of 96 selected printouts of coal data were supplied to other agencies upon request along with 114 coal samples.

Necessary software modifications have been established for conversion from a PDP-9 to a PDP-8 minicomputer system for pyrite chord size analysis using the Rapid Scan Automated Reflectance Microscope System. Experimental programming to improve the resolution of petrographic components in the coal reflectrogram has been outlined, although implementation of these ideas has been delayed because of inadequate hardware facilities. Preliminary tests on the new Leitz 1350 heating stage of the hot-stage microscopy system have been completed. Work continues on evaluation of heating-rate controller systems.

A number of hardware additions have been made to the Digital Equipment Corporation PDP-8 minicomputer system in order to adapt the Penn State/ERDA Coal Data Base to a minicomputer environment. A set of administrative control programs have been written to monitor the status of all coal samples from the time of collection through the time of completion of all analytical work.

Construction of the pressurized laminar-flow isothermal reactor of Facet IV-A continues with delivery now expected around June, 1977. The University has placed the construction of an appropriate building facility very high on its priority list and is seeking funding. Preliminary work on more extensive and detailed modeling, intended to complement further experimental studies on the mechanism of gasification in a combustion pot has led to grant awards from The Pennsylvania Science and Engineering Foundation and the Caterpillar Tractor Corporation for applications of modeling to the design of industrial shaft gasifiers. A series of experiments in the combustion pot is currently underway using a coke provided by the Koppers Company. Initial studies have indicated that reactivity of this coke is substantially different from that of the coke tested previously.

Under Task 24 the reactor system and mass spectrometer are being calibrated with various hydrocarbon gases and solids to determine residence times and cracking pattern characteristics for use with coal pyrolysis product analysis. In addition, the rapid heating (of the order of 8000°C/sec) of a North Dakota lignite (PSOC-246) in a nitrogen atmosphere has been studied using a 2 in. ID laminar flow isothermal furnace. The effect of residence times up to about 1 sec at maximum temperature (808°C) on changes in coal properties and weight loss has been studied. For residence times up to about 1 sec the lignite is found to undergo a monotonic decrease in weight and a monotonic increase in specific surface area and density. Changes which the coal undergo during the heating and cooling periods are negligible compared to changes produced while at maximum temperature. As shown during this quarter, the extent of burnoff of PSOC-246 (270 x 400 mesh) in air greatly exceeds weight loss due solely to pyrolysis in nitrogen.

A technical report is in preparation entitled, "The Characteristics of Chars Produced by Pyrolysis Following Rapid Heating of Pulverized Coal".

Under Facet IV-B a series of thirteen samples were prepared from a lignite char by (1) depositing different amounts of carbon by the cracking of methane, and (2) activation of the raw and carbon deposited samples to different levels of carbon burn-off. Methanol and water densities of various samples were found to be very close to the helium densities.

Use of small angle x-ray scattering techniques continues in the characterization of pore structures of a series of chars. Parameters have been determined which are used to calculate total surface area and characteristic dimensions of pores and matter between pores.

Studies of carbon deposition from the cracking of methane into pores of a lignite char have shown that carbon deposition occurs at a significant rate at temperatures between 815 and 855°C. Removal of inorganic impurities from the char by acid-washing significantly reduces the extent of carbon deposition. The maximum amount of carbon deposition is much less than the amount of open pore volume which is potentially available to accommodate carbon. Carbon deposition reduces surface area and pore volume of the lignite char, as well as accessibility of methane into the internal pore structure.

Differential scanning calorimetry has been established as a fast experimental technique for characterization of carbonaceous materials. The effect of different variables such as the level of burn-off, particle size, and bed height of the carbon, as well as reaction temperature and flow rate on the heat of chemisorption of oxygen on Saran carbons has been examined. The existence of different kinetic stages corresponding to adsorption on different active sites are indicated. The chemisorption process is associated with a physical adsorption process at lower reaction temperatures and a gasification reaction at higher temperatures. At 100°C, the extent of physical adsorption and gasification reaction are minimal.

Possible catalytic activity of major minerals formed in coals for the cracking of methane has been studied. Siderite and calcite were found to catalyze the cracking reaction. No catalytic activity was observed for dolomite, pyrite, illite, quartz, rutile, and kaolinite. Gypsum was found to react with methane although no carbon deposition was observed.

Two additional technical reports are near completion covering work which was scheduled under Facet IV-B. They are entitled: "Effects of Heat Treatment Conditions on Reactivity of Chars in Air" and "The Effect of Cation Exchange on the Subsequent Reactivity of Lignite Chars to Steam".

The experimental work performed to date under Facet V-A on combustion of chars and anthracite has recently been analyzed within the framework of a simple radiative theory of flame propagation and the existing computer model has been used to investigate the effect of fuel particle density changes.

The combustion characteristics of coal-oil-water-air mixtures are being studied using a 2.0 million Btu/hr hot-wall type furnace with water tubes to simulate thermal loading. The effect of the water and coal additions on the heat transfer and pollution characteristics of No. 2 fuel oil have been studied. The addition of water in fuel oil reduces the useful heat output of the furnace. Water additions also reduce the amount of excess air at various smoke levels, although the reduction of excess air at the smoke point (0% smoke) is not significant. As up to 5 percent coal is added to the oil-water-air emulsion, a rise in furnace efficiency is attributed to increasing flame emissivity without significant changes in the excess air requirements for complete combustion. Beyond that level of coal additions a decline in furnace efficiency is attributable to the attenuation of the radiation from the walls in transmission through the flame. Trends in gas temperatures substantiate this argument.

FACET I-A: SAMPLE COLLECTION AND SEAM CHARACTERIZATION

COAL SAMPLING

During the period of this report a sampling trip was made to the Broad Top Coal Field in Bedford County, Pennsylvania where three coal seams were sampled. A large channel sample (PSOC-615) and three subsection samples (PSOC-616 through 618) were taken from the Kelly seam; a channel sample (PSOC-619) of the Barnett seam was obtained; and a channel sample (PSOC-620) and two subsection samples (PSOC-621 and 622) of the Twin seam were taken.

A drill core of the Wall Coal seam from Campbell County, Wyoming was received from the Denver Office of the USGS. The first sample from our sampling subcontract with Texas A & M University was received in this quarter and consisted of a large channel sample and three subsection samples from the lignite seam mined near Darco, Texas. We have also received twelve drums of coal from our subcontract with Southern Illinois University. These samples consist of a channel sample from two different coal seams and three subsection samples from each seam.

FACET I-B: COAL CHARACTERIZATION

COAL CHARACTERIZATION

Maceral and reflectance analyses were performed on one sample supplied by another ERDA Contractor (POC-299). Maceral analyses were completed on 125 PSOC samples and reflectance analyses on 122 PSOC samples, plus three older samples were reread using the brown coal analyses technique. Ultraviolet light analyses were performed on PSOC-431 and 434. In addition, 93 samples were sent out for standard chemical analyses; polished blocks were made of 98 samples and the Vickers microhardness determined on these blocks. Also, 15 FSI analyses and Gray-King coke tests were run and 46 Hardgrove grindability determinations were made. Splits from 34 new coals, and additional material from 11 coals already supplied, were sent to the Mineral Constitution Laboratories for elemental and mineralogical analyses.

The Mineral Constitution Laboratories at Penn State determine the elemental and mineralogical composition of coals contained within the Penn State/ERDA Coal Sample Bank. Currently, major and minor element data (Si, Al, Fe, Ca, Mg, Mn, Na, K, and Ti) are being obtained from high temperature coal ashes (750°C) using a plasma emission spectrometer while trace element data are obtained from the same ash using both the plasma spectrometer (for Ba, Cu, Sr, V, Zn, and Zr) and a standard d.c. arc emission spectrograph (for Ag, Be, Bi, Ce, Co, Cr, Ga, Ge, La, Mo, Nb, Ni, Pb, Se, Sn, Y, and Yb). Additionally, rubidium and mercury are being determined by atomic absorption spectrophotometry on the high temperature ash and as-received coal respectively, where uranium and phosphorus are determined by neutron activation and x-ray fluorescence on the as-received coal. Quantitative mineralogical analyses are being obtained from low temperature coal ashes using x-ray diffraction (for calcite, pyrite, and quartz) and infrared techniques (for kaolinite and gypsum). Qualitative x-ray diffraction and infrared scans of each sample are also taken to determine the presence of any phases not looked at on a routine quantitative basis. A form of normative analyses is being used to estimate the content of clays other than kaolinite (for example, montmorillonite, illite, and mixed-layer clays). A general flow diagram of the entire analytical procedure is presented in Figure 1.

As of March 3, 1977, 443 coal samples have been received. Of these, 354 have been ashed at 750°C and 181 have been processed through the low temperature asher. Major and minor element data have been obtained for 88 PSOC coals while trace element data is available for 168. Mineralogical analyses have also been completed on 60 LTA's.

RAPID SCAN AUTOMATED REFLECTANCE MICROSCOPE SYSTEM

Several new data acquisition algorithms for pyritic sulfur analysis have been conceived during this period. These will be implemented on the new Digital Equipment Corporation PDP-8 computer, which will replace an older model,

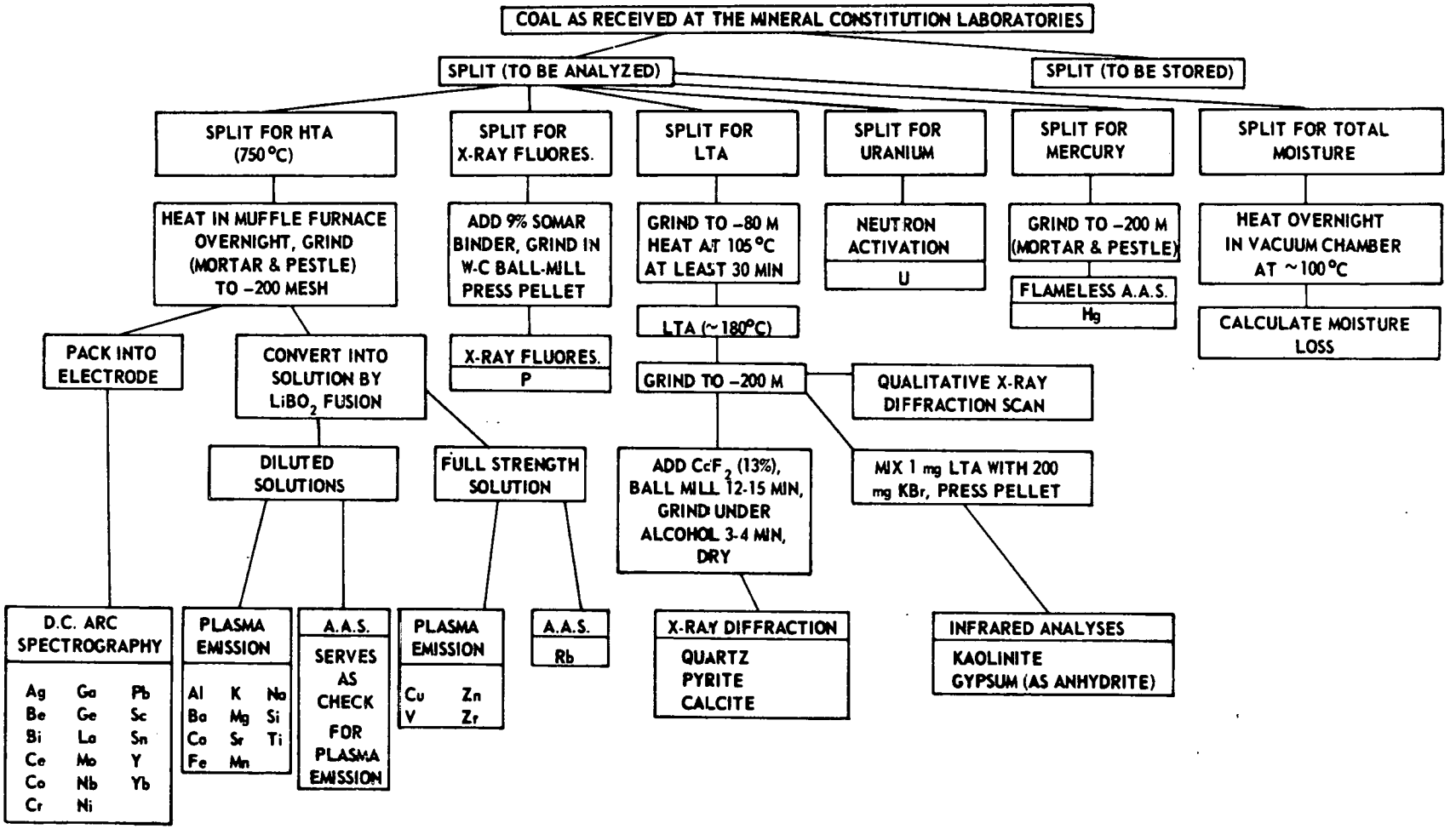

Figure 1 ANALYTICAL SCHEME FOR PSOC COALS AT THE PENN STATE MINERAL CONSTITUTION LABORATORIES

the PDP-9, in the system. A larger memory, disc storage, and multiple language capabilities are features which make the PDP-8 a more flexible tool for the purpose of coal characterization. Once the necessary software modifications have been effected, future work will be directed toward analyzing samples from various stations in a coal preparation plant. Any observable changes in the pyrite chord size distribution will be studied with the intent of increasing the efficiency of pyrite removal.

The resolution of the coal reflectogram has beem examined with the purpose of gaining additional quantitative data. It has been determined that in order to apply advanced mathematical modeling techniques, the reflectogram will have to resolve the different petrographic components. Several approaches have been studied in an attempt to realize the best improvement. It is believed that advanced programming of the data acquisition mode of operation will yield the most apparent improvement. The programming has been flowcharted, but its implementation has been delayed by the availability of the necessary facilities. Future work will involve implementing and experimenting with this type of advanced system.

HOT-STAGE MICROSCOPY

The initial testing phase has been completed for the new Leitz 1350 heating stage of the hot-stage microscope system. Two tests, to evaluate the system standardization, were run during this time. The melting point standards employed in these tests were tin (231.9°C) and aluminum (660.1°C). The initial tests indicate that the system is operating properly under normal control. Work is continuing on evaluating heating-rate controller systems. The current system will need significant overhaul and modification for adaptation to the new heating stage. These modifications are being studied at this time. Future work will involve attempting to interface the available controller with the new heating stage. Improvements in the microscope illumination system will also be investigated.

FACET I-C: SAMPLE BANK OPERATION, MAINTENANCE, AND DEVELOPMENT

SERVICE TO OTHER AGENCIES

During this period, the number of requests from other research agencies for samples and data has continued to be large. A total of 96 selected print-outs of coal data were supplied to other agencies along with 114 coal samples.

Fifty samples were sent to North Dakota State University and three samples were supplied to the Materials Research Laboratory at The Pennsylvania State University. Gulf Research and Development Corporation was sent seventeen samples while twenty-nine samples went to Florida Atlantic University and one large sample was supplied to the Institute of Gas Technology. The Atlantic Research Corporation was provided with one sample, twelve samples went to the Jet Propulsion Laboratory at the California Institute of Technology, and one sample was sent to the Aerospace Corporation.

FACET I-D: PENN STATE/ERDA COAL DATA BASE

COAL DATA BASE ACTIVITY REPORT

The Penn State/ERDA Coal Data Base was further expanded this quarter to include data on 43 additional coal samples, bringing the total number of coals in the data base to 379. Existing files were updated for newly acquired trace element and major element data.

The following hardward additions have been made to the Digital Equipment Corporation PDP-8 minicomputer system.

1) A floating point processor to increase the speed and precision of the present computing facilities.

2) A large capacity DEC RK05 disk drive to store large quantities of information on-line in order to meet the needs of the expanding coal data base.

3) A selectable high, low speed Vadic modem to enable communication with external terminals and other computer installations.

4) A Houston plotter to facilitate computerized graphical representations of data.

5) Two DEC VT-52 video terminals have been installed. One terminal is dedicated to remote date entry and administrative management use. These terminals also have graphics capabilities.

The following administrative control programs have been added to the system. They have been designed so that an untrained operator can use them in a prompting question-answer mode. The purpose of these programs is to monitor the status of all coal samples from the time of collection through the time of completion of all analytical work. The following program options are available.

1) List coal samples giving seam name, county, state, and sample type.

2) List coal samples giving seam name, collectors I.D., and sample type.

3) List which analyses have been completed on a selected range of coal samples.

4) List which analyses have work pending on a selected range of coal samples.

5) List completion dates for selected analyses.

6) List information available on an individual coal sample.

7) Insert additional data into the coal sample inventory.

8) Edit and update existing coal sample inventory.

9) Printout the number of samples on which work has been completed for any selected work unit (analysis) for any selected time period.

FACET IV-A: REACTOR DEVELOPMENT AND OPERATION

EVALUATION OF THE GASIFICATION POTENTIAL OF COALS

Introduction

Construction of the pressurized laminar flow isothermal reactor continues and delivery is expected about June, 1977. Since the University's attempts to provide an appropriate building facility have not materialized yet, it is apparent that the reactor will be installed in the Combustion Laboratory building as originally anticipated. The temporary location will permit the use of the reactor under all operating conditions except those utilizing hydrogen and similar highly reactive gas atmospheres. The research conducted at the temporary location should not lack in importance, for there are many experiments which should be run in inert atmospheres. Aside from the expected requirement of familiarizing the operating personal with the equipment, the reactor must first be characterized in a number of operational and response aspects. Subsequently, a wide spectrum of important experiments in inert atmospheres will entail original ventures into the pressurized regime. These will extend to the limit cases of total combustion.

Experimental

During this reporting period the cold flow similation investigation of the dependence of the pressure drop through the bed as a function of particle size and flow rate has been completed. In addition, combustion pot experiments were carried out using one size grade of coke obtained from the Koppers Company at three different air flow rates.

During this reporting period, the cold flow measurements described in the last quarterly report were extended to both smaller and larger particle sizes. Figure 2 illustrates the variation of pressure drop per unit length ($\Delta P/L$) with velocity. For the range of particle sizes investigated (0.59 in. to 1.375 in.) pressure drop per unit length is proportional to the square of the mean superficial velocity $\bar{U}_S$, leading to the conclusion that the flow is turbulent over the entire range of conditions investigated. For a flow through a fixed bed of solid particles, the total external surface area per unit bed volume for spherical particles is given by $A_S = 6(1 - \varepsilon)/d$, where the bed porosity is a function of the diameter, d. Toward using the pressure drop through the bed as an index of the specific surface area A_S, the variation of the mean pressure gradient divided by the squared superficial velocity with the inverse squared particle diameter was plotted, and found to be linear.

If the pressure drop and flow velocity are obtained continuously during each combustion pot experiment, one can estimate the variation of the mean particle diameter. To obtain the external surface area, A_S, for which the value of the bed porosity is required, experiments to determine the variation of ε with particle size will soon be undertaken.

A new series of experiments in the combustion pot is currently underway using a coke obtained from the Koppers Company. The results for these tests will be compared with those reported previously for Penn State foundary cokes,

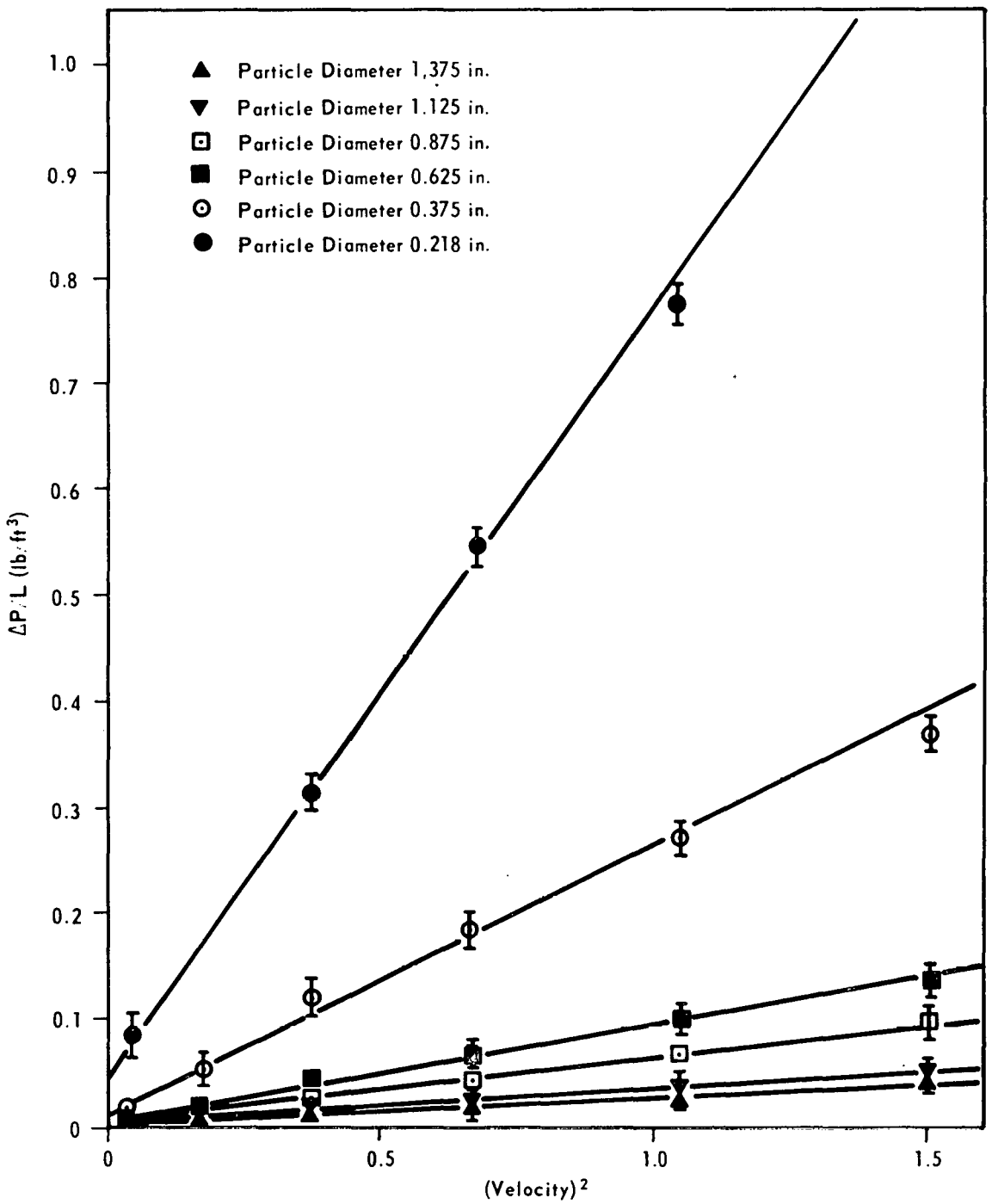

Figure 2 VARIATION OF PRESSURE DROP WITH SQUARE OF VELOCITY

and both cokes will be characterized by such tests as proximate analysis and determination of calorific values.

The new coke was size graded to 0.875 in. (± 0.125 in.), and experiments have been carried out in the manner established previously. An initial study of the dependence of the kinetic constants on the type of fuel was carried out by using the experimental results obtained with this one particle size. Kinetic coefficients were obtained from a log/linear plot (Figure 3) of the concentration term $[(O_2 + CO_2/2)/(1 + CO_2)]$ versus time.[1] Previous analysis[1] has shown that the kinetic constant n_1, in the combustion region, is proportional to $(\text{velocity})^{0.7}$. To test this behavior, Figure 4 is a log/log plot of n_1 (initial slopes of the curves in Figure 3) against velocity. The solid lines in the figure are least squares fit to the experimental points and the dashed lines are the 0.7 slopes. The reactivity of the present coke is substantially different from that of the coke tested previously. The study of the influence of particle size on the gasification behavior of this coke will be continued.

EFFECT OF HEATING RATE AND SOAK TEMPERATURE ON VOLATILE MATTER RELEASE

Introduction

Further theoretical analysis was performed using the coal particle pyrolysis model. The reactor system and mass spectrometer are being calibrated with various hydrocarbon gases and solids to determine residence times and cracking pattern characteristics for use with coal pyrolysis product analysis.

Experimental

Extensive computer runs were performed for the coal pyrolysis model. The following parameter set was used as a reference in these runs:

Physical parameters -- Particle size: 100 μm
Driving temperature: 1273.0°K

Chemical parameters -- Activation energy: 25.0 kcal
Pre-exponential: 10^7 sec^{-1}
Heat of reaction: -250.0 cal/g

Using this set as a reference the following parameter variations were made to determine their effect upon the mode of pyrolysis, that is, whether it is expected to be volumetric or shrinking-core in nature:

Physical parameters -- Particle size: 25 μm to 500 μm
Driving temperature: 873.0°K to 1873.0°K

Chemical parameters -- Activation energy: 20.0 kcal to 30.0 kcal
Pre-exponential: 10^7 sec^{-1} to 10^{13} sec^{-1}
Heat of reaction: 0.0 cal/g to -1000 cal/g

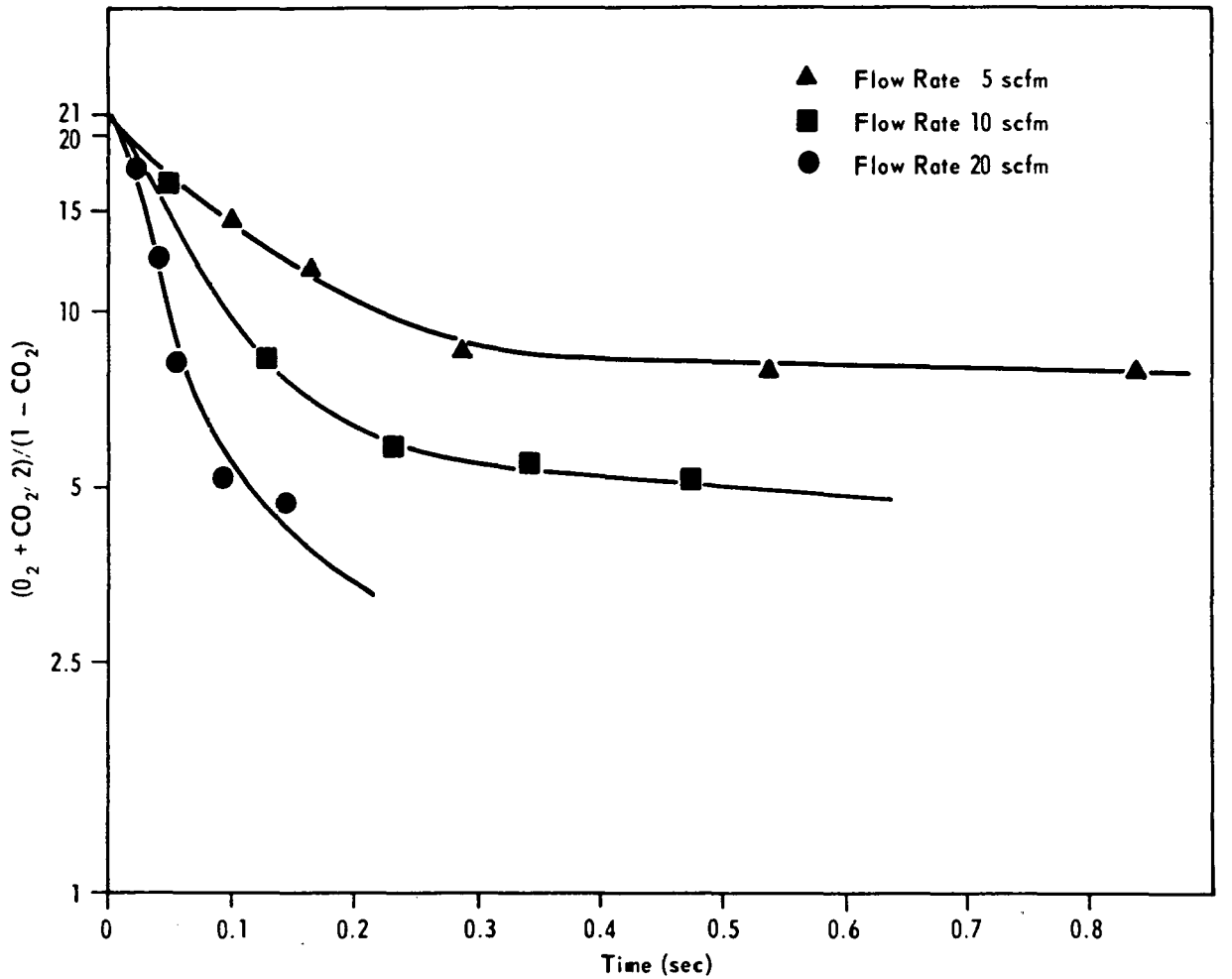

Figure 3 VARIATION OF $(O_2 + CO_2/2)/(1 - CO/2)$ WITH TIME FOR 0.865 IN. COKE PARTICLES

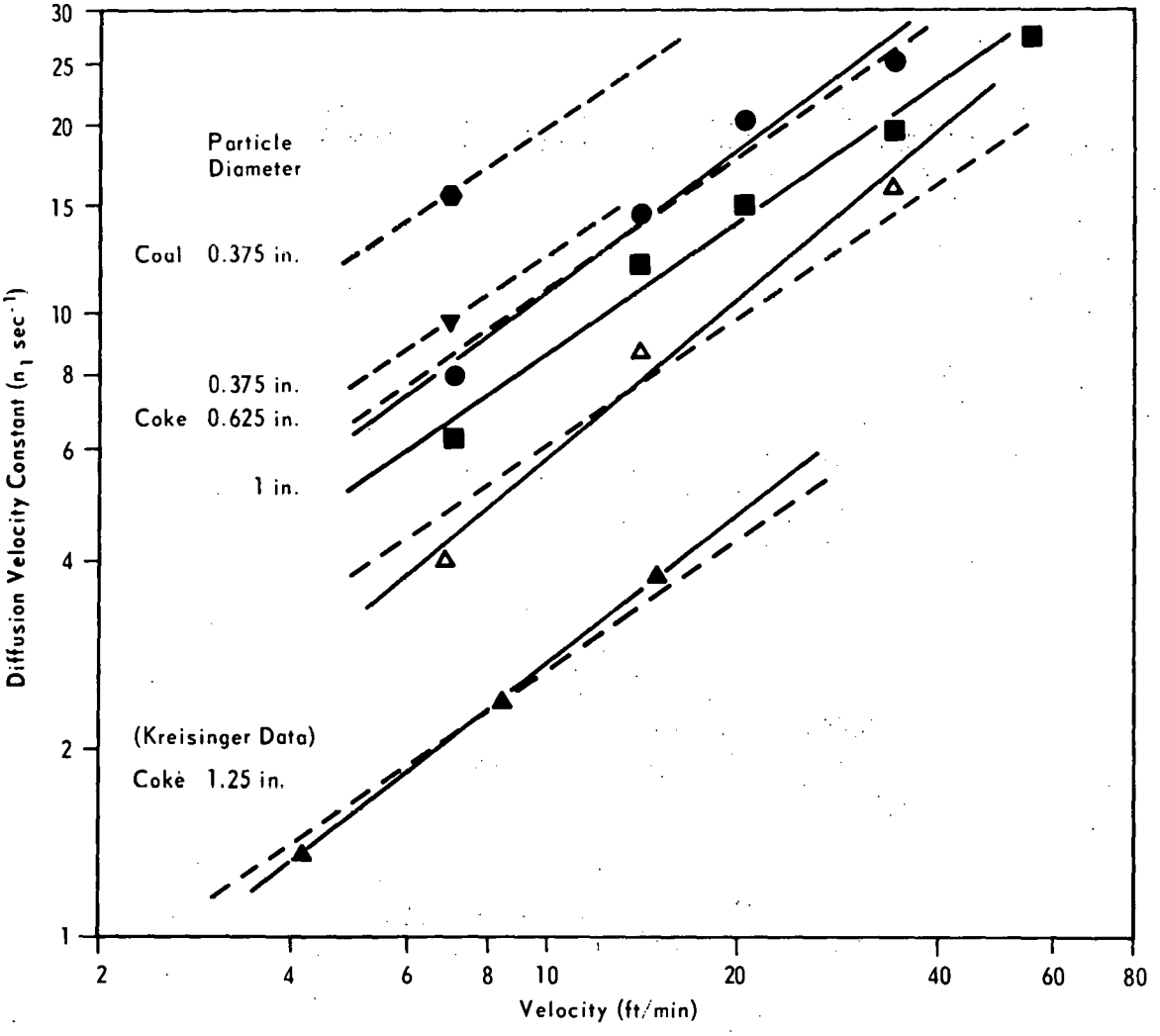

Figure 4 VARIATION OF DIFFUSION VELOCITY CONSTANT n_1 WITH VELOCITY. SOLID LINES ARE LEAST SQUARES FIT; DASHED LINES ARE SLOPE 0.7. DATA FROM KREISINGER (16) ARE ALSO INCLUDED (BOTTOM LINE)

Graphical temperature and remaining pyrolytic material profiles were obtained at various reaction times. These results are being prepared for a special report. Included herein are two graphs indicating the type of results obtained (see Figures 5 and 6). In this case the effects of varying particle size upon the mode of pyrolysis are indicated.

The split ratio of the sampling valve of the mass spectrometer was determined to insure that only a small amount of the total flow (less than 1 part in 1000) was being diverted to the mass spectrometer. This will allow, given that the total flow and pressure are known, the quantity of each of the hydrocarbon gases in the main stream to be determined. The flow through the splitter was in the Poseville regime. In this regime the flow through the splitter is proportional only to the pressure gradient. Since the stream is at atmospheric pressure, the flow into the mass spectrometer will be constant.

Trial napthalene vaporization runs in the reactor were made with the mass spectrometer as a detector. The data revealed: (1) that the concentration of the hydrocarbons in the helium carrier gas was at least four orders of magnitude above the detectable limit of the mass spectrometer; (2) the residence time of a known mass of hydrocarbon vaporizing; and (3) the amount being detected. The implication is that the coal pyrolysis product analysis will have equally successful results.

The cracking patterns and sensitivities of various hydrocarbon gases were examined by the mass spectrometer. This enables the identification and quantitative analysis of pyrolysis products to be made.

The next step in developing the theoretical model is to include the effects of mass transport. Completion of calibration of the mass spectrometer and reactor systems will enable quantitative analysis of coal pyrolysis runs. The results of the runs will be correlated to the theoretical model to determine kinetic parameters.

CHARACTERISTICS OF CHARS PRODUCED BY PYROLYSIS AND COMBUSTION FOLLOWING RAPID HEATING OF PULVERIZED COAL

Introduction

Characteristics of chars produced in various atmospheres (for example, nitrogen, air, and carbon dioxide) are being studied, using the same laminar flow isothermal furnace which has been described in previous progress reports. During this quarter work has been conducted using nitrogen and air as a pyrolysis and combustion medium, respectively, and one size grade (270 x 400 mesh) of a North Dakota lignite (PSOC-246) as the starting parent coal.

Experimental

The pyrolysis of PSOC-246 was conducted in nitrogen at 808°C (experimental conditions follow). The ultimate analysis of the North Dakota lignite was contained in the last quarterly report.[2] The proximate analysis of its 270 x 400 mesh size grade is given in Table 1. A study of the particle size distribution of this size grade using the Rosin-Rammler method gives a particle weight mean size of 42 μ (that is, $\bar{x}$ = 42 μm), see Table 1.

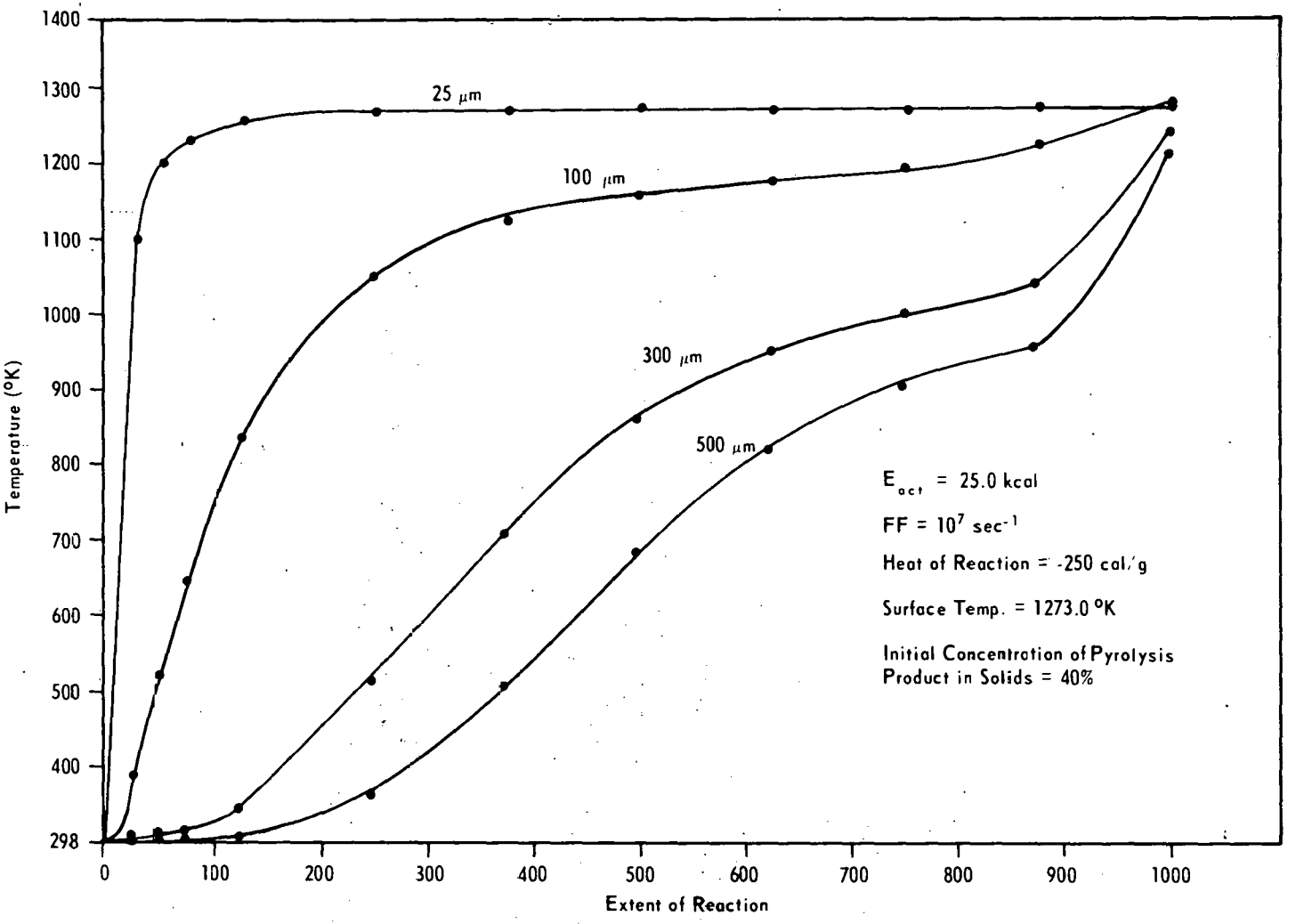

Figure 5 TEMPERATURE AT PARTICLE CENTER DURING REACTION FOR VARIOUS PARTICLE SIZES

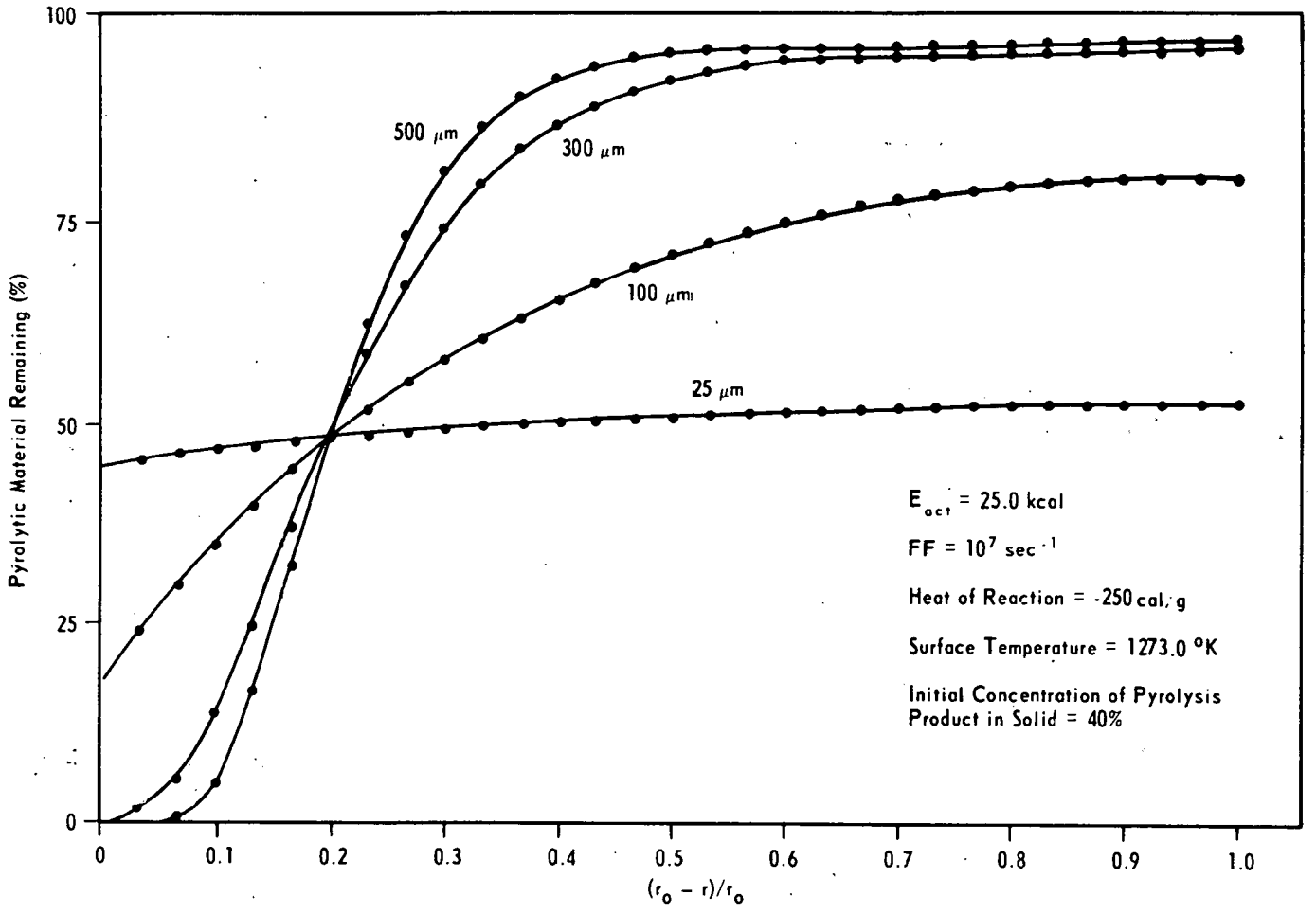

Figure 6 PYROLYTIC MATERIAL PROFILES AT 50 PERCENT REACTION COMPLETION FOR VARIOUS PARTICLE SIZES

Table 1. Analytical Data on Montana Lignite (PSOC-246)

(a) Proximate Analysis (at 270 x 400 Mesh)

	As Received	Dry	Dry, ash-free
Moisture	14.6	-	-
Ash	6.7	7.8	-
Volatile Matter	37.9	44.6	48.2
Fixed Carbon	40.8	47.8	51.8

(b) Weight Mean Size (at 270 x 400 Mesh)

$\bar{x}$ x 42 μm

(c) Equivalence Ratios (ϕ) for Combustion in Air

Coal Feed Rate (g/min)	Theoretical Air Required for Complete Combustion (ϕ = 1.0)	Air Used During Experiment
1.0	5.3 ℓ(STP)/min	31.7 ℓ(STP)/min (ϕ = 0.17)
1.4	7.4 ℓ(STP)/min	31.7 ℓ(STP)/min (ϕ = 0.23)

Most of the experimental conditions given in the previous reports were maintained, namely (1) total flow rate of nitrogen = 31.7 ℓ(STP)/min, (2) temperature = 808°C, (3) char collector probe suction rate = 14 ℓ(STP)/min, (4) pressure = atmospheric. Coal feed rates of 0.5 and 1 g/min were used. Under these conditions the total residence time of particles in the furnace reaction zone of 30.5 cm in length is 300 msec.

The chars collected at various positions in the reaction zone were analyzed for proximate ash contents (see Table 2). Two runs were made using a coal feed rate of 1 g/min, and one run was made using a coal feed rate of 0.5 g/min. Table 2 shows that ash contents in the resulting chars were independent of these feed rates. Hence, the three values of ash (A') were used to determine at 95 percent confidence limits the average value of ash ($\bar{A}'$) at each position. This value was, in turn, used as a tracer to determine weight loss to 95 percent confidence limits.

The resulting weight loss as a function of residence time is given in Figure 7. The error bars depict the 95 percent confidence limits with which the points were measured. Note should be taken that the first two points in this figure show negative values of apparent weight loss, because the values of ash in these chars (Table 2) are consistently lower than that of the original material (Table 1). This shows a net loss of ash in the early stages of pyrolysis, an effect which is overcome by greater extent of pyrolysis in the later stages of the process. This effect, which was not encountered in the study of larger particle sizes of PSOC-246[3], is thought to be due to the fact

Table 2. Proximate Ash Contents of PSOC-246 Chars Produced in Nitrogen and Air at 808°C at Different Coal Feed Rates into the Furnace Reaction Zone*

Distance	Time	Pyrolysis in Nitrogen				Combustion in Air	
(cm)	(msec)	$A'_{1.0}$	$A'_{1.0}$	$A'_{0.5}$	$\bar{A}'$	$A'_{1.0}$	$A'_{1.4}$
7.6	75	7.60	7.51	7.40	7.50 ± 0.25	7.73	7.84
11.4	112	7.63	7.62	7.59	7.61 ± 0.05	7.73	8.06
15.2	150	7.64	7.96	7.82	7.81 ± 0.39	8.10	8.74
19.1	188	8.0	8.10	8.02	8.04 ± 0.13	9.29	10.10
22.9	225	8.38	8.27	8.33	8.33 ± 0.14	14.81	10.86
26.7	264	8.91	8.60	8.70	8.74 ± 0.39	23.38	17.64
30.5	300	9.78	9.52	9.76	9.69 ± 0.36	28.62 29.10	25.52

*A' stands for proximate ash content on dry basis (these values are averages of two or three determinations in each case). The subscript indicates the coal feed rate (for example, $A'_{1.0}$ is the ash content for a coal feed rate of 1 g/min). Weight loss (ΔW) and burn-off (η) were determined using these values of ash as tracers.

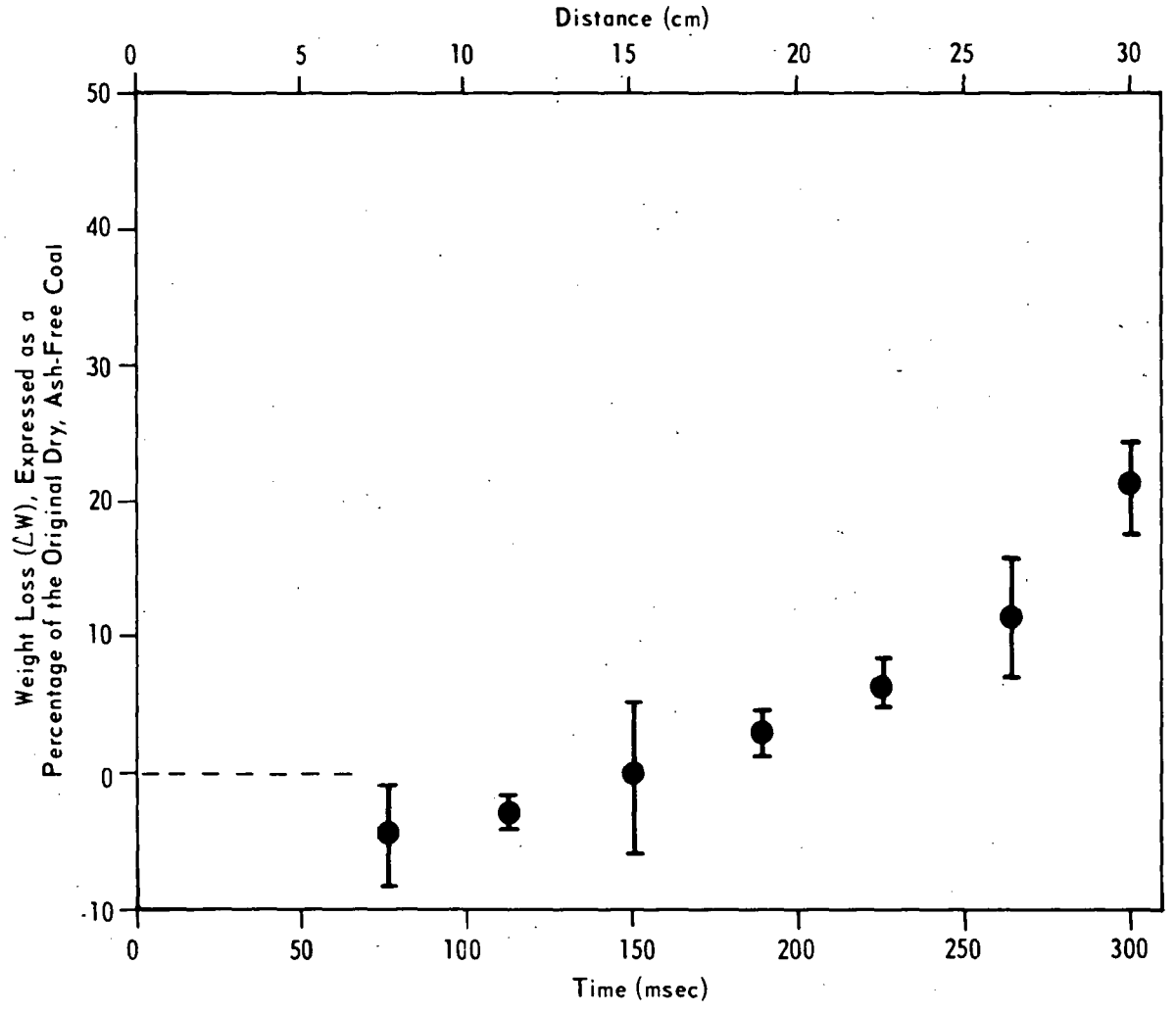

Figure 7 VARIATION OF WEIGHT LOSS WITH RESIDENCE TIME FOR PSOC-246 COAL (48.2% VM, $\bar{x}$ = 42 μm)

that discrete mineral particles are easily separable from the coal particles in finely ground coal.[4] In this case the separation was thought to occur in the screw feeder and/or in the furnace as the particles were flowing downward in dilute suspensions. Hence, cold runs were made, keeping the other experimental conditions constant. The proximate ash contents of the sample collected in the funnel (which is located just below the screw feeder) and in the cyclone (after a transit distance of 30.5 cm) were determined. The results show that ash content in the sample collected in the cyclone is greater by about 1 percent than that of the sample collected in the funnel. The difference in ash content between the sample from the hopper and the funnel is indistinguishable. The value of ash given in Table 1 is the average between the ash contents of samples from the hopper, the funnel, and the cyclone. While these results show that there is indeed separation between discrete mineral particles and coal particles, it is unclear where some of the mineral particles go during pyrolysis. The statistical significance of this ash separation is under further investigation. However, it is noteworthy to mention that Kobayashi and others[5] also found that for bituminous coal at low weight losses the ash tracer technique gave negative apparent weight losses.

The experimental conditions which follow apply to the combustion of PSOC-246 in air at 808°C. From knowledge of the ultimate analysis of PSOC-246[2] it was possible to calculate the theoretical amount of air required for complete combustion of the coal. Table 1 shows that 5.3 and 7.4 l are required for a stoichiometric combustion of 1 g and 1.4 g of PSOC-246, respectively. Under these conditions, the equivalence ratio (ϕ) is unity. However, because 31.7 ℓ(STP)/min were fed into the furnace, these conditions gave equivalence ratios of 0.17 and 0.23 for a coal feed rate of 1 g/min and 1.4 g/min, respectively, which are highly lean mixtures. In any event, complete combustion also depends on other factors, for example, particle size distributions, temperature/time history of the particles in the reaction zone, and diffusion limitations. Actually, complete combustion in this study is undesirable since the study is aimed at the determination of the physical characteristics of the chars produced. Under the experimental conditions given above, it was possible to collect sufficient amounts of chars at different positions in the reaction zone. The proximate ash contents of these chars are given in Table 2. Again these values were used as tracers to determine the extent of burn-off. The results are plotted in Figure 8. Here, again, slightly negative values of burn-off are encountered in the early stages of combustion. The explanation given in the foregoing section apparently applies also in this case. This figure shows that a total burn-off of nearly 80 percent occurs in 300 msec, as compared to about 21 percent weight loss in the case of pyrolysis.

Pyrolysis in nitrogen and combustion in air of other size grades of PSOC-246 will be conducted at 808°C in the laminar flow isothermal furnace. Selected chars from these studies (including some from this report) will be systematically characterized for specific surface areas, densities, total open pore volumes and porosities.

A 2 in. ID high temperature furnace is currently being built at the Combustion Lab. This furnace will allow these studies to be conducted at temperatures up to about 1000°C. This is quite important in measuring kinetic parameters (such as activation energy, frequency factor, and velocity constant), and the maximum potential weight loss in the case of pyrolysis.

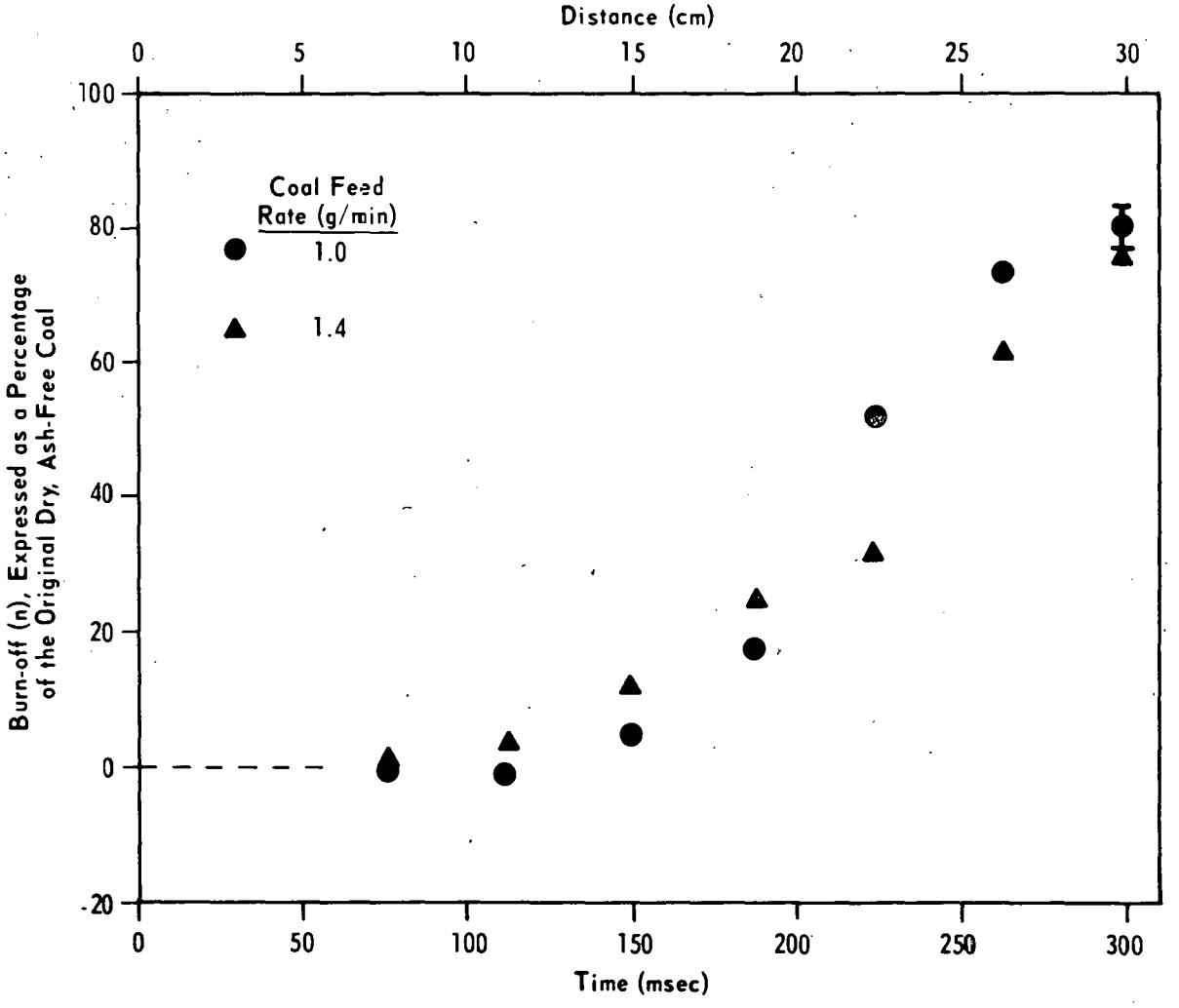

Figure 8 VARIATION OF BURN-OFF WITH RESIDENCE TIME FOR PSOC-246 COAL (48.2% VM, $\bar{x}$ = 42 μm)

FACET IV-B: COKES AND CHARS

METHANOL AND WATER DENSITIES OF COALS AND CHARS

Water densities were determined on seventeen coals varying in rank from LV bituminous to lignite. The coals were ground and 40 x 70 mesh fractions used for density measurements. Water densities were determined at 25°C using the pycnometer technique. For each sample, the water densities were determined after different intervals of contact time. The densities showed a drift with time, but for each sample constant limiting values were obtained within five days. The 'constant' densities for different samples are listed in Table 3. With the exception of coal PSOC-268, the water densities of the remainder of the samples are invariably higher than the corresponding helium densities.

It has been reported that for lower rank coals water densities are higher than the helium densities whereas for higher rank coals the water densities are lower. The higher values were attributed to imbibing and/or specific interactions with the oxygen-containing functional groups present on coal surfaces[6]. The lower water densities were attributed to the extensive hydrophobic character of higher rank coals as a result of which air present in the pores is not completely displaced by water[6,7]. The latter explanation is not supported by the fact that the water densities of chars, which are devoid of essentially all volatile matter and are, therefore, hydrophobic in nature, have been reported in the previous progress reports to be in close agreement with the helium densities.

Ettinger and Zhupakhina[7] have reported that water densities of coals determined in the presence of a wetting agent are in excellent agreement with the helium densities. We propose to follow their technique; the two sets of densities for different coals will be compared. Further, it has been shown that particle densities of coals determined by the 'silanization' technique are very close to those calculated from the geometric measurements. Particle densities of a number of coals of different rank will be determined by mercury displacement as well as by the silanization technique.

SMALL ANGLE X-RAY STUDIES ON COAL CHARS

Introduction

The major objectives of this investigation are to characterize the pore structures of a series of chars by means of small angle x-ray scattering (SAXS). Methods of characterizing pore structures which involve fluid penetration are somewhat limited for chars prepared at temperatures about 1000°C. It is known, from density data, that these materials do contain extensive pore systems. However, measurements of surface area often yield extremely low, unrealistic values. The reason for these underestimated values is that these materials contain cavity/aperture pore systems in which the apertures act as barriers for penetrating fluids. The diffraction of x-rays at small angles arises from the presence of heterogeneities in solid matrices. In the case of porous chars the heterogeneities stem from the presence of pores. Hence, from analyses of SAXS

Table 3. Helium and Water Densities of Coals

PSOC Sample No.	ASTM Rank	C (%, daf)	Ash (Wt %, daf)	Density, mmfb(g/cm^3) Helium	Water
318	LV	89.5	6.52	1.348	1.526
236	MV	89.4	8.02	1.293	1.301
135	MV	88.3	4.96	1.335	1.350
254W	MV	87.1	5.90	1.300	1.465
268	HVA	85.9	5.09	1.390	1.371
281	HVB	83.2	10.58	1.310	1.344
223	HVB	81.2	3.72	1.296	1.400
238	HVA	79.4	9.46	1.271	1.364
221	HVA	79.3	5.67	1.305	1.476
212	HVC	79.0	2.65	1.322	1.432
288	HVC	78.2	9.01	1.320	1.363
312	HVC	77.7	6.61	1.294	1.327
233	HVC	77.3	9.09	1.333	1.463
230	Sbb-B	75.2	9.16	1.242	1.328
248	Sbb-A	75.1	2.93	1.466	1.556
242	Sbb-B	73.8	5.88	1.483	1.648
246	Lignite	70.9	9.70	1.387	1.563

data it is possible to characterize the pore structure without being limited by the size of apertures.

In previous reports we have detailed much of the theoretical background for interpretation of SAXS data. It has been shown that from a primary SAXS parameter 'ℓ_m' (range of inhomogeneity) the pore structure of a char can be defined in terms of three parameters. These secondary parameters are: surface area, a characteristic dimension of pore size, and a characteristic dimension of the carbonaceous material between pores. The estimation of these parameters requires a knowledge of the volume fraction of pores, 'c', contained in each sample. Previously, we estimated 'c' from density data and found that for a series of demineralized coal chars there are systematic changes in pore structure which are functions of rank of the parent coal and heat treatment temperature. It was concluded, therefore, that SAXS can be an extremely useful tool for characterizing chars. Although the density method of estimating 'c' is adequate for determining total porosity it does tend to overestimate the volume fraction of pores which contribute to SAXS. Hence, it was decided that attempts be made to determine 'c' directly from the SAXS profiles. Such an approach would lead to a significant refinement of our data.

Experimental

The evaluation of the volume fraction of pores directly from the SAXS data requires that absolute intensity data be taken. To obtain such data a calibrated intensity standard must be used. Such a calibrated sample (a

platelet of polyethylene) was obtained. This standard is placed in the primary x-ray beam and the resulting intensity, at a specific angle, is measured. This value is then used to normalize the scattered intensities of the char sample under investigation. It can be shown that

$$c(1-c) - kQ' \qquad (1)$$

where c = volume fraction of pores
Q' = normalized invariant
k = constant.

Thus, by evaluation of Q' and the appropriate constants, 'c' can be found. At the present time this approach is being applied to the ten char samples which have been previously described.[8] Early results indicate that 'c' values determined by this method are somewhat smaller than those determined by density measurements.

The volume fraction of pores in the series of chars will be completed. Detailed comparisons will then be made between the secondary parameters calculated by both the absolute intensity and density methods.

EFFECT OF CARBON DEPOSITION ON THE POROSITY AND REACTIVITY OF CHARS

Introduction

Deposition of carbon has a large and lasting adverse effect on the subsequent reactivity of the char to air. This has been attributed both to a decrease in active surface areas and deactivation of catalytic inorganic impurities due to coating with carbon. Deposited carbon is much less reactive to air than the lignite char.

Experimental

This report describes the effect of carbon deposited within the pore volume of the lignite char on subsequent reactivity in air.

Reactivity of chars to 1 atm of air before and after carbon deposition was determined in the TGA unit. About 4 mg of sample were taken in a platinum pan. It was ascertained in a few preliminary experiments that under the chosen experimental conditions, char reactivity was independent of bed height (weight). That is, resistance for diffusion of reactant gas molecules down through the bed was minimal. Prior to making reactivity runs, the system was flushed with nitrogen (300 cm^3/min) for 30 min to displace the air present. The sample was then heated to the desired gasification temperature at a rate of 10°C/min. Heating was continued at this temperature until the sample weight became constant. Following this, nitrogen was replaced by air at the same flow rate. The decrease in sample weight during gasification was recorded continuously as a function of time.

Burn-off curves for the raw and acid-washed chars before and after carbon deposition are plotted in Figures 9 and 10. Each curve has an initial

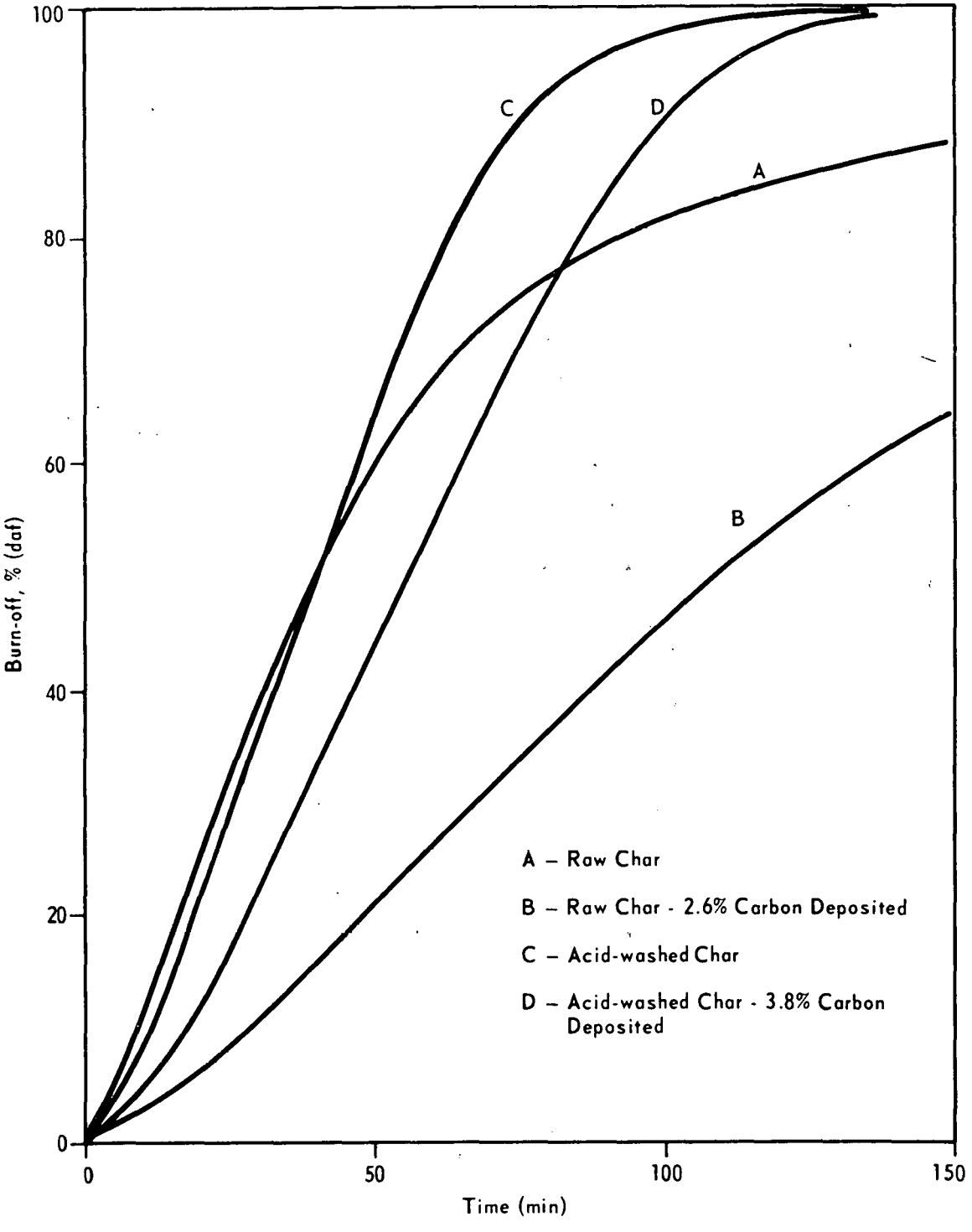

Figure 9 BURN-OFF CURVES IN AIR AT 375 °C FOR 855 °C RAW AND ACID-WASHED CHARS BEFORE AND AFTER CARBON DEPOSITION

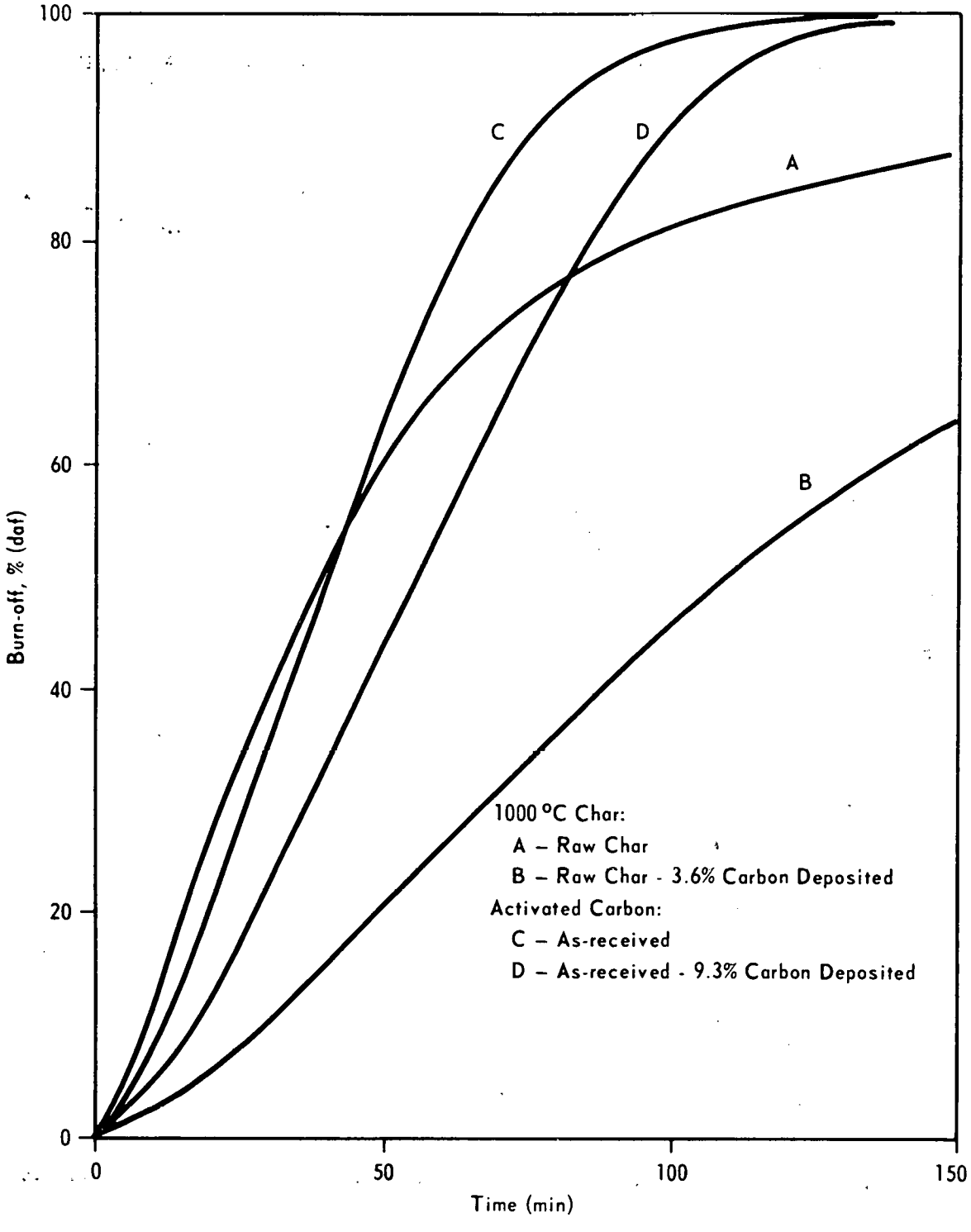

Figure 10 BURN-OFF CURVES IN AIR AT (i) 375 °C FOR RAW AND CARBON DEPOSITED 1000 °C LIGNITE CHAR, AND (ii) 500 °C FOR AS-RECEIVED AND CARBON DEPOSITED ACTIVATED CARBON

induction period. Thereafter, an essentially rectilinear region associated with a maximum reactivity is found. Finally, the reactivity decreases continuously until the sample has been gasified. The reactivity parameter (R) was calculated from the following equation:

$$R = \frac{1}{W_o} \cdot \frac{dW}{dt} \qquad (2)$$

where W_o is the starting weight of the char on a dry, ash-free (daf) basis and dW/dt is the maximum rectilinear rate of weight loss. In the present study, time corresponding to 50 percent burn-off (τ) has also been used as an index of char reactivity. Obviously, the smaller the τ value, the larger will be the char reactivity. Values of R and τ for various samples are listed in Table 4.

Considering the plots in Figures 9 and 10 and R and τ values in Table 4, it is seen that the 1000°C char is significantly less reactive than the 855°C char. The reactivity decreases appreciably upon carbon deposition as well as upon mineral matter removal (by acid washing). Both the R and τ values indicate that the acid-washed char following 3.8 percent carbon deposited is about one-eighth as reactive as the corresponding raw char.

For comparison, results on an activated carbon were also determined. It was found that the reactivity of the activated carbon to air was too slow to measure at 375°C. Therefore, reactivity was measured at 500°C. Reactivity plots (Figure 10), as well as the R and τ values (Table 4) for the as-received and 9.3 percent carbon deposited samples, indicate that the reactivity of the carbon also decreases following carbon deposition.

As is seen from Figure 9, 2.6 percent, by weight, deposited carbon on the 855°C lignite char affects the whole burn-off curve. That small amounts of carbon deposited have such pronounced effects on lignite char reactivity is instructive. Two extreme situations can be considered. On the one hand, the deposited carbon can be much more reactive to air than is the lignite char carbon. In this case, in the limit, the initial burn-off will be totally accounted for by the deposited carbon and the original microporous structure in the lignite char quickly restored. Experimental results show clearly that this was not happening. On the other hand, the deposited carbon can have a much lower reactivity than the base lignite char carbon. Surface area development by char gasification resulting in the enlargement of apertures (and increasing gasification rates) will be small since deposited carbon will block apertures. In fact, experimental results suggest that the truth lies more closely to the latter extreme situation. Surface area development in the char as a result of gasification is sharply reduced by prior carbon deposition, as discussed earlier. As discussed in the last progress report, burn-off of the 855°C raw char to about 30 percent burn-off increases nitrogen surface area from 241 m^2/g to about 695 m^2/g. By contrast, burn-off of the 2.5 percent carbon deposited raw char sample to about 30 percent only increases the nitrogen surface area from 33 m^2/g to about 160 m^2/g. It is, therefore, clear that carbon deposition on the lignite char is undesirable if one wishes to maximize surface area development and concurrent char reactivity.

Table 4. Reactivity Results for Various Chars and Activated Carbon Samples

Sample	Reactivity Parameter (R) ($mg\ hr^{-1}\ mg^{-1}$)	τ (min)
	855°C Char	
Raw char	1.21	28
Raw char: 2.6% carbon deposited	0.85	47
Acid-washed	0.45	99
Acid-wached: 3.8% carbon deposited	0.16	228
	1000°C Char	
Raw char	0.87	39
Raw char: 3.6% carbon deposited	0.31	108
	BPL Activated Carbon	
As-received	0.85	39
As-received: 9.3% carbon deposited	0.62	56

Reactivity of carbons is dependent upon, among other variables, the concentration of active sites in the carbon. The concentration increases with decrease in crystallite size, decrease in crystallite orientation, and increase in defect concentration in the basal plane. Since pyrolytic carbons normally show reasonable crystallite alignment with their basal planes parallel to the substrate surface on which deposition has occurred, it is concluded that the deposited carbon has a smaller active site concentration than the turbostratic lignite char carbon. It should be possible by tracer studies, using tagged carbon-13 in the methane, to quantitatively follow the relative reactivities of carbon-12 in the lignite char and carbon-13 in the deposited carbon.

With the submission of this report the work on carbon deposition of chars will be discontinued for the time being.

CHEMISORPTION OF OXYGEN ON CARBONACEOUS SOLIDS

Introduction

Differential scanning calorimetry (DSC) has been established as a fast experimental technique for characterization of carbonaceous materials. The effect of different variables such as the level of burn-off, particle size, and bed height of the carbon, as well as reaction temperature and flow rate on the heat of chemisorption of oxygen on Saran carbons has been examined. The existence of different kinetic stages corresponding to adsorption on different active sites is indicated. The chemisorption process is associated with

a physical adsorption process at lower reaction temperatures and a gasification reaction at higher temperatures. At 100°C, the extent of physical adsorption and gasification reaction are minimal.

Experimental

The DSC and TGA techniques have been used to study the thermal effects involved during chemisorption of oxygen on Saran carbons. In addition, total area accessible to oxygen during chemisorption was determined mass-spectrometrically.

The procedure for determination of active surface area by the TGA technique follows. A known amount of the sample was evacuated at room temperature down to 10^{-4} torr. The sample was heated at 20°C/min up to 950°C and then held isothermally at this temperature for 48 hr. During the first few hours of the hold period the decomposition products increased the pressure up to 10^{-1} torr, after which it dropped down to 10^{-4} torr and remained constant for 24 hr. The sample was cooled to room temperature and nitrogen was introduced inside the reactor. The sample was heated to 100°C in a nitrogen flow at the rate of 45 cm^3/min. The temperature was held constant for 30 min. Thereafter, oxygen was introduced to replace nitrogen at the same flow rate. The amount of oxygen chemisorbed was recorded as a function of time. Table 5 lists the amounts of oxygen chemisorbed on the oxygen-activated Saran sample (63.8% burn-off). It is noteworthy that 50 percent of the total oxygen chemisorption occurs during the first hour. Since the increase in weight due to chemisorption was negligible between 40 and 48 hr, the experiment was terminated after 48 hr. That is, it was assumed that in 48 hr the carbon surface was essentially "saturated" with chemisorbed oxygen.

A value of 8.3 $Å^2$ was taken as the average area occupied on the carbon surface by a chemisorbed oxygen atom. This value was used to calculate the extent of surface coverage (Table 5). The heat treatment conditions prior to chemisorption employing the mass-spectrometric technique were essentially the same as those used during the TGA runs. However, there was one noticeable exception. In the mass spectrometer, the sample was evacuated down to 10^{-7} torr at 950°C for 48 hr. It was then cooled under vacuum to 100°C. Oxygen was introduced at 1 atm. After 48 hr, oxygen was pumped out at 100°C. The sample temperature was raised stepwise to 950°C to desorb the chemisorbed oxygen. A liquid nitrogen trap was used to freeze out the evolved carbon dioxide. From the total amounts of carbon monoxide and carbon dioxide evolved, the amount of oxygen chemisorbed at the carbon surface was calculated to be 16.61 mg/g carbon. This value is higher than that determined by the TGA unit (Table 5), obviously because the outgassing conditions were more stringent in the mass spectrometer unit. Therefore, it was decided to use the value of 16.61 mg oxygen/g carbon for calculating the total active surface area accessible to oxygen during chemisorption. This area was calculated to be 26.0 m^2/g, compared to the total area (as determined by the Polanyi-Dubinin equation from carbon dioxide adsorption at 298°K) of 850 m^2/g. That is, the active area represents only 3.05 percent of the total area.

In order to investigate the dependence of ΔH on surface coverage, it was essential to conduct experimental runs with the DSC and TGA units under identical

Table 5. Oxygen Chemisorption on the Activated Saran Carbon at 100°C

Time	Oxygen Chemisorbed (mg/g carbon)	Area Covered by Chemisorbed Oxygen (m^2/g carbon)	Fractional Surface Coverage, θ
2 min	2.923	4.566	0.233
6	3.842	6.002	0.307
10	4.396	6.867	0.351
15	4.763	7.441	0.380
20	5.039	7.872	0.402
25	5.223	8.159	0.417
60	6.326	9.882	0.505
2 hr	7.245	11.318	0.578
4	8.348	13.041	0.666
10	9.083	14.119	0.721
15	10.002	15.625	0.798
20	10.737	16.773	0.857
25	11.289	17.636	0.901
30	11.840	18.496	0.945
35	12.208	19.071	0.975
40	12.484	19.503	0.997
48	12.527	19.570	1.000

experimental conditions. The first step was directed to explore the pretreatment parameters that might possibly affect the amount of oxygen chemisorbed at the carbon surface. The DSC technique, being much faster than the TGA technique, was used for these exploratory studies. The carbon sample was evacuated at room temperature, flushed with nitrogen, heated at a rate of 20°C/min up to 600°C, and then held at 600°C for different soak times. The chemisorption runs were thereafter conducted at 100°C in the manner described in previous progress reports.

The effect of soak time at 600°C on heat of oxygen chemisorption, Q (cal/g carbon), is illustrated in Figure 11. For zero soak time, the value of Q at any reaction time is higher than that obtained when soak time is 5 hr. A similar behavior (trend) was also observed during the TGA runs; at a particular reaction time the amount of oxygen chemisorbed decreased as the soak time increased (Figure 12). This indicates that deactivation of active sites is more pronounced with longer soak times. Values of ΔH at selected adsorption times are given in Table 6. These values are scattered around an average value of 70.4 kcal/mole. Thus, although soak time at 600°C affects the amount of oxygen chemisorbed at 100°C, it does not affect the value of ΔH.

In order to calculate surface coverage over which the constant value of ΔH is obtained, a long term experiment was performed with the TGA unit. During

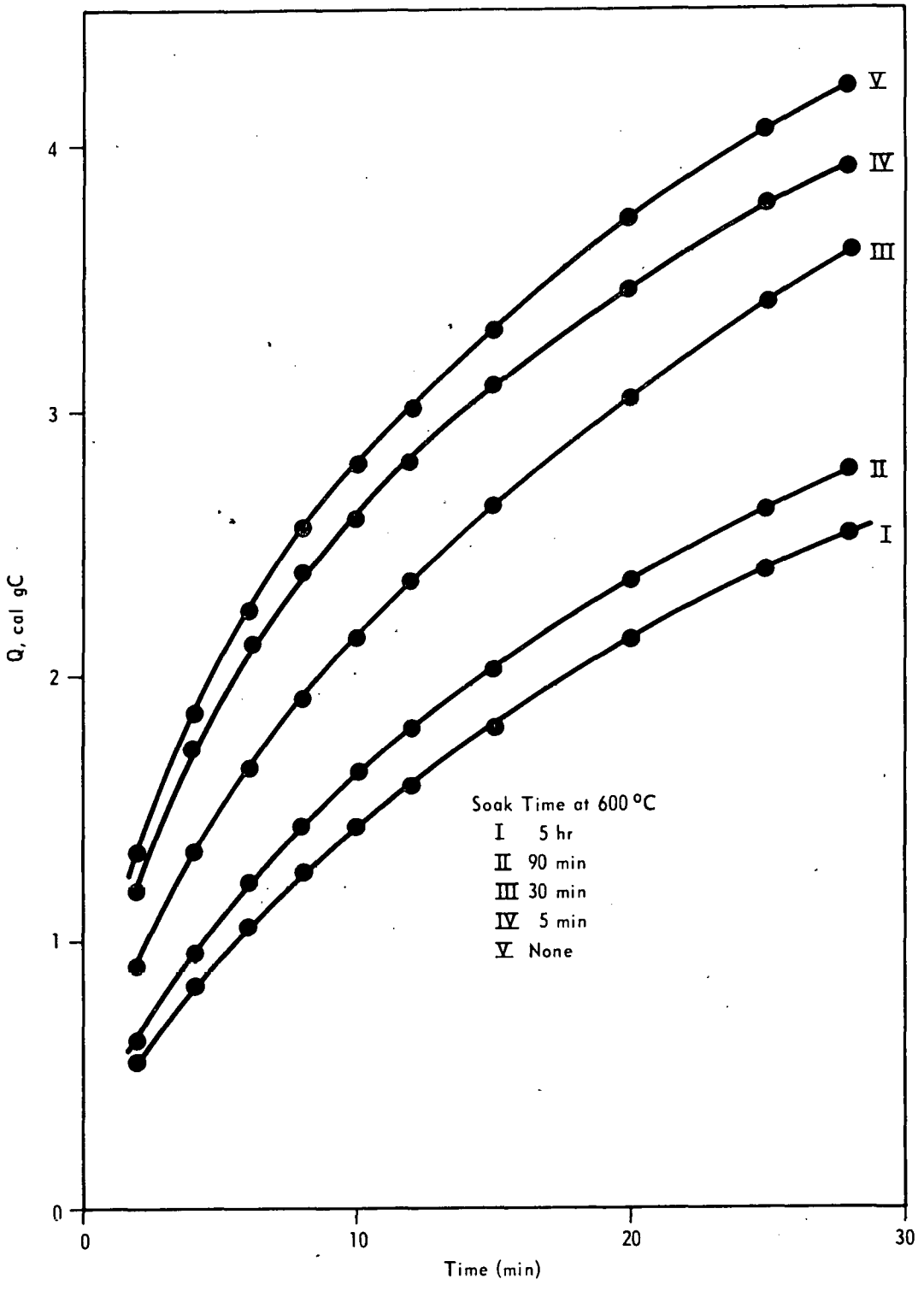

Figure 11 DEPENDENCE OF Q ON SOAK TIME AT 600°C PRIOR TO OXYGEN CHEMISORPTION ON SARAN CARBON AT 100°C

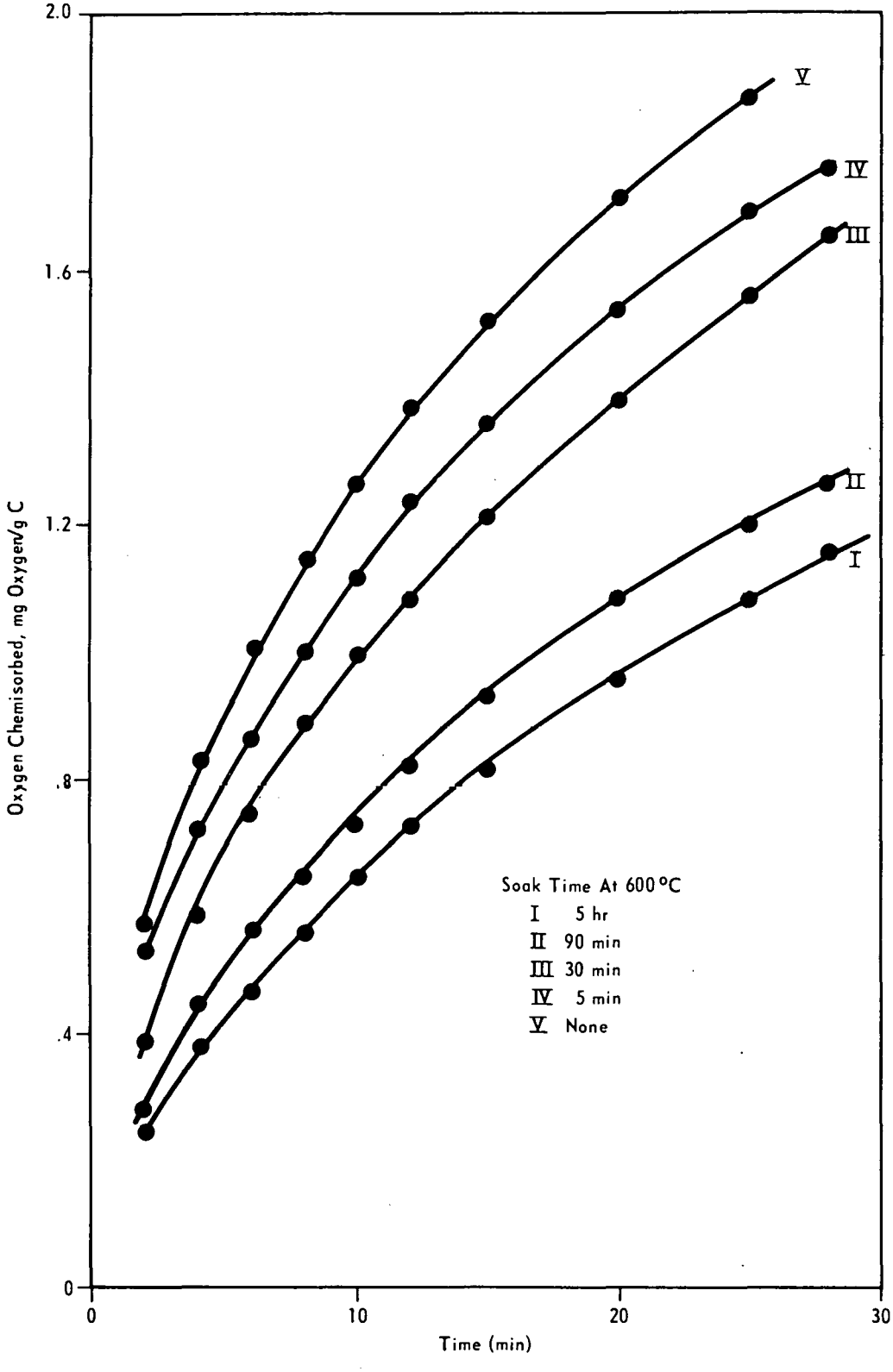

Figure 12 DEPENDENCE OF WEIGHT CHANGES DURING CHEMISORPTION ON SOAK TIME

Table 6. Values of ΔH (kcal/mole) for Oxygen Chemisorption on Saran Carbon at 100°C

Adsorption Time, min	Soak Time at 600°C				
	Zero	5 min	30 min	90 min	5 hr
6	69.8	72.0	71.9	69.4	68.7
10	71.1	71.0	69.2	71.4	71.2
15	69.8	71.1	70.8	69.8	71.6
20	70.8	69.5	70.3	69.7	71.5
25	68.6	70.1	70.3	70.1	71.3
28	70.3	69.4	69.8	72.2	70.8

the pretreatment of the sample, it was kept at 600°C for 30 min. The sample was cooled to room temperature in a nitrogen atmosphere, held at 100°C for 1 hr. Oxygen was then introduced. The amount of oxygen chemisorbed was monitored for 36 hr, after which additional weight increase due to chemisorption was negligible. The sample was cooled, evacuated, flushed with nitrogen, and again subjected to the same pretreatment procedure, that is, heat treatment up to 600°C. A second adsorption run at 100°C was then made. The adsorption-desorption cycle was again repeated on the same sample after which a third adsorption run was made. Table 7 lists the amounts of oxygen uptake for the three successive adsorption cycles at different reaction intervals. The total amount of oxygen uptake determined mass-spectrometrically, that is, 16.61 mg oxygen/g carbon, was used to calculate the fractional surface coverage, θ. For example, at the end of the first cycle, the total amount of oxygen chemisorbed is 5.788 mg/g carbon. Thus, the difference 16.610 - 5.788 = 10.822 mg oxygen/g carbon is not desorbed during the pretreatment conditions followed in this study, that is, heat treatment up to 600°C and soak time at 600°C of 30 min. Therefore, during the first cycle the total amount of oxygen present on the surface after 2 min is 0.387 + 10.822 = 11.209 mg/g carbon. The fractional surface coverage, θ, is therefore, given by:

$$\theta = \frac{\text{oyxgen present on the surface}}{16.61} = \frac{11.209}{16.610} = 0.675 \qquad (3)$$

The maximum surface coverage at the end of the first adsorption run was calculated to be 0.746. Thus, the results of the present investigation show that in the surface coverage range (θ) 0.675 - 0.746, the values of ΔH are almost constant at 69.2 to 71.9 kcal/mole (Table 6) and are essentially independent of soak time at 600°C prior to oxygen chemisorption at 100°C.

The effect of heating rate and maximum heat treatment temperature used for 'cleaning' the carbon surface prior to oxygen chemisorption, bed height (bed weight) and oxygen flow rate on Q will be investigated. In order to measure ΔH as a function of surface coverage, TGA runs at 100°C will be conducted for extended periods of time following cleaning of the sample in a nitrogen flow at different heat treatment temperatures.

Table 7. Effect of Adsorption-Desorption Cycles on Fractional Surface Coverage

Adsorption Time	Adsorption Cycle 1		2		3	
	W*	θ**	W*	θ**	W*	θ**
2 min	0.387	0.675	0.307	0.729	0.168	0.820
10 min	1.011	0.712	0.840	0.761	0.512	0.841
28 min	1.562	0.746	1.306	0.789	0.948	0.867
1 hr	2.113	0.779	1.773	0.817	1.259	0.885
36 hr	5.788	1.000	4.806	1.000	3.161	1.000

*W (mg oxygen/g carbon)
**Fractional Surface Coverage

CATALYTIC ACTIVITY OF MINERALS FOR THE CRACKING OF METHANE

Results of x-ray studies pertaining to those minerals which catalyze the cracking of methane, namely, siderite, calcite, and gypsum, are presented.

For x-ray studies, we needed relatively larger quantities of samples than those which could be handled in the TGA unit. Therefore, the following preparative procedure was followed. About 1 g of mineral sample was taken in a quartz boat which was then placed in a tube furnace. The system was flushed with nitrogen for 30 min after which heating was started at the rate of 10°C/min. In those cases where the interest was to find out the chemical changes undergone by the minerals upon heating to 900°C in nitrogen, the samples were soaked at 900°C for 30 min and then cooled to room temperature in nitrogen. When the products of cracking were to be studied, nitrogen was replaced by a mixture of nitrogen and methane at a total pressure of 1 atm and a methane partial pressure of 50 torr.

X-ray diffraction profiles revealed that, following heat treatment at 900°C in nitrogen, siderite is converted essentially to wustite (FeO); very feeble peak intensities corresponding to α-iron were also observed. It was reported by us in the last progress report that in the TGA runs when nitrogen is replaced by the nitrogen-methane mixture at 900°C, FeO is quantitatively reduced to iron. This was confirmed by x-ray studies.

In order to find out the products formed by the cracking of methane, FeO (derived from siderite at 900°C) was treated with the methane-nitrogen mixture for 24 hr. The products identified by x-ray studies were α-iron and carbon. Considering that the carbon was formed at 900°C, it was found to be highly crystalline having an interlayer spacing of 3.371Å and an average crystallite height, L_c, of 500Å.

It may be recalled that in the TGA runs calcite was found to lose carbon dioxide in a nitrogen atmosphere in the temperature range 500-750°C, producing calcium oxide. Further, in the methane-nitrogen mixture, a slow, continuous

weight increase was observed. In contrast to sharp (002), (100), (102), and (004) peaks found for the carbon deposited on iron (derived from siderite), only a very broad (002) diffraction peak was found for this carbon. This indicates that it has a very small crystallite size. X-ray diffraction peaks were also present for calcium oxide.

When gypsum ($CaSO_4 \cdot 2H_2O$) was heated to 900°C in nitrogen, calcium sulfate (anhydrite) and calcium oxide were identified by the x-ray studies. However, following treatment with methane-nitrogen mixture, calcium sulfate, calcium oxide, and calcium sulfide were identified; no surface deposition of carbon was observed.

With the submission of this report, the work on methane cracking over minerals will be discontinued. The results obtained will be reported in the form of a publication.

COMBUSTION OF CHAR AND ANTHRACITE COAL IN LARGE UTILITY BOILERS

Introduction

Two manuscripts which summarize and analyze the experimental and theoretical work accomplished to data have been prepared and submitted to Combustion Science and Technology for publication. The titles and authors are: "Flame Stabilization of Low Volatile Fuels" by J.G. Cogoli, D. Gray, and R.H. Essenhigh; and "Computer Modelling of a Plane Flame Furnace Firing Low Volatile Fuels" by J.G. Cogoli and R.H. Essenhigh. New developments resulting from the preparation of these two papers will be briefly summarized here.

Experimental

The previously reported char combustion data have been analyzed with respect to an existing flame propagation theory.

Established simple theory[9] shows that in a radiation stabilized flame particle heating rate is primarily a function of the radiative flux from the flame, and of the optical depth of the unburned cloud or, equivalently, the radiation absorption coefficient, k_o.

The absorption coefficient can be expressed as a function of the ambient dust cloud concentration, D_o, the mean initial particle radius, a_o, and of the particle density, σ, thus:

$$k_o = 3D_o/4a_o\sigma \qquad (4)$$

Since clouds of a given fuel/air ratio have about the same cloud concentration and particle density for all coals, they will also have about the same radiation absorption coefficient or optical depth if ground to the same size, unless the particles of some fuels swell or shatter before ignition. Unless there is some swelling or shattering, significant differences in ignition behavior, therefore, are not readily attributable to variations in absorption coefficient.

The flame temperature can be shown[9] to enter the problem by an equation for the limiting time-to-ignition $(t_i)_L$, thus:

$$(t_i)_L = (4a_o\sigma/3I_f)(T_i - T_o)[c_d + c_p(\rho_o/D_o)] \qquad (5)$$

where T_i and T_o are the ignition and ambient temperatures respectively, c_d and c_p are the mean specific heats of dust and gas respectively, ρ_o is the STP gas (air) density, and I_f is the black body radiative flux from a flame system at some mean flame temperature, T_f. In this expression, only T_i and I_f are parameters with much potential for variation between fuels. With a high temperature coefficient for the heterogeneous (ignition) reaction, and with bituminous coal ignition starting at about 1000°C, an ignition temperature for an anthracite or a char would not be expected to exceed 1400 or 1500°C, with 1200 to 1300°C

as a more reasonable expectation. Reactivity should not, therefore, affect the ignition time by more than 10 or 20 percent. There is inherently more scope for influence on $(t_i)_L$ by the flame temperature, T_f, or radiation flux, I_f, but the numerical values are informative. A doubling of ignition time would be achieved with about a 20 percent drop in flame temperature, which is not excessive, but if T_f for bituminous coal is 1500°C, or 1800°K, a 20 percent drop would reduce T_f to 1150°C which would be below the expected ignition temperature for the anthracite.

These theoretical expectations can be set against some experimental results obtained on Howard's furnace[10-13] nearly 10 years ago using a coal char obtained from the IGT gasification process. On the basis of the above argument, heating rates of the char were expected to be somewhat comparable to those of the bituminous coal with peak flame temperatures somewhat lower. The results were the inverse of expectation: flame temperatures were comparable, if not higher, and heating rates were drastically lower, with ignition distances for similar input velocities about an *order of magnitude* greater, or heating rates nearly an order of magnitude lower.

The effect of increasing air flow rate has been documented experimentally in previous publications[10-14], and will be now closely analyzed. In each case the fuel supply rate was kept constant and the air supply rate was increased. Under these conditions, the dust cloud concentrations or fuel/air ratio dropped as the air rate was increased. With the Bureau of Mines char there was only sufficient sample for two runs, executed at an extremely fuel rich and at a considerably fuel rich condition (air *deficiencies* being approximately 75% and 15%). All other experiments were carried out at air rates of 8.8, 11.6, 13.8, and 17.8 scfm and fuel rates of 12.5 ± 2.5 lb/hr, corresponding to excess air levels of approximately -47 percent, -30 percent, -16 percent, and + 20 percent. The FMC char could not sustain flames at the two highest air flow rates.

The temperatures generally rise with increasing air, but the clearest behavior is the effect on the flame front. In its simplest terms, increasing the air flow rate simply blows the flame downstream.

The increase in ignition distance, L_i, however, does not necessarily increase the ignition time, t_i, since we may define a mean velocity, $\bar{v}$, between entry and ignition such that: $L_i = \bar{v}\, t_i$; and appropriate plots of L_i against v_o (as a first approximation to $\bar{v}_i$) showed an approximate linearity consistent with an approximately constant t_i. The linearity was only approximate, however, and it justified further examination of the data in the case of chars E1 and E2, these being the only two chars for which sufficient data were available. Equation 5, it may be recalled, is the expression for the limiting time-to-ignition at small t_i. If t_i is not small, it is shown[14] that the relation between coal inlet velocity, v_o and ignition time can be written

$$v_o = s_o[1 - \exp(-k_o v_o)(-t_i)] \qquad (6)$$

where s_o is the maximum or limiting flame speed, given by

$$s_o = I_f/(T_i - T_o)(D_o\, c_d + \rho_o\, c_p) \qquad (7)$$

[In Equation 6, t_i is inherently negative because of choice of axes.]

To test this equation, values of t_i were obtained from the measured ignition distances and input velocities corrected for the increase due to temperature. Reviewing the exponent term of Equation 6, this is a function of three variables, t_i, v_o, and D_o (in k_o), where D_o falls as the air velocity is increased at constant fuel feed rate. A direct test of Equation 6 was not possible since insufficient parameters were known. It was tested, however, by graphical iteration, by plotting v_o against $(D_o v_o t_i)$, which was found to have a (1 - exp) form with sufficient curvature to estimate the upper flame speed. Equation 6 can be written in the alternative form

$$- (D_o v_o t_i) = (4a\sigma/3) \ln (1 - v_o/s_o) \qquad (8)$$

and Figure 13 is the plot of $-(D_o v_o t_i)$ against $\ln (1 - v_o/s_o)$. The data, though sparse, are consistent with this equation representing a straight line through the origin. The slope of the mean line through the origin yields a value for the radius, a, which is about 1/3 of the estimated mean radius. We can obtain a closer agreement if we assume in the original analysis[14] that there is sufficient scattering and transmission of radiation for the whole surface to be absorbing instead of just the projected area. In that case, the slope would be $(4a\sigma)$ which yields a value of about 20 μ for the radius or 40 μ for the diameter.

Use was made of the result of the preceding section that enabled us to calculate the group $(k_o v_o t_i)$ for all experimental runs and, hence, to use Equation 6 to determine s_o, the limit flame speed, as the slope of the radius vector from the origin on a plot of v_o against $[1 - \exp(k_o v_o t_i)]$. From Equation 7, it is then possible to say that

$$I_f = \sigma_b \bar{T}_f^4 = [s_o(D_o c_d + \quad_o c_p)](T_i - T_o) \qquad (9)$$

where σ_b is the radiation constant.

We are therefore able to relate a possible range of radiation fluxes (I_f) or flame temperatures (T_f) to a range of ignition temperatures (T_i) for all the fuels, with the ranges also bounded by certain conditions.

Table 8 summarizes the essence of the results reported above using the ignition distance at 8.8 scfm air flow and 12.5 lb/hr fuel as the standard basis of comparison. As observed earlier, and as Table 8 shows explicitly, the fuels evidently belong to one of two extreme "reactivity" groups with ignition distance or times differing by an order of magnitude. Particle size can account for 10 or 20 percent variation in flame front position for the low reactivity fuels, but it barely affects the high reactivity fuels. Input velocity increases ignition distance roughly in proportion, but ignition time for a given fuel which takes input velocity into account is approximately constant. To a better approximation it obeys Equation 6.

The fuels used in the experimental studies were found to have densities at two different levels, a factor of two apart. The densities of the bituminous coal, the anthracite, and the low reactivity chars were close to 1.3 g/cc (80 lb/cu ft), and the high reactivity chars were close to half this value at 0.65 g/cc (40 lb/cu ft). All calculations were therefore carried out at one or the other of these two values.

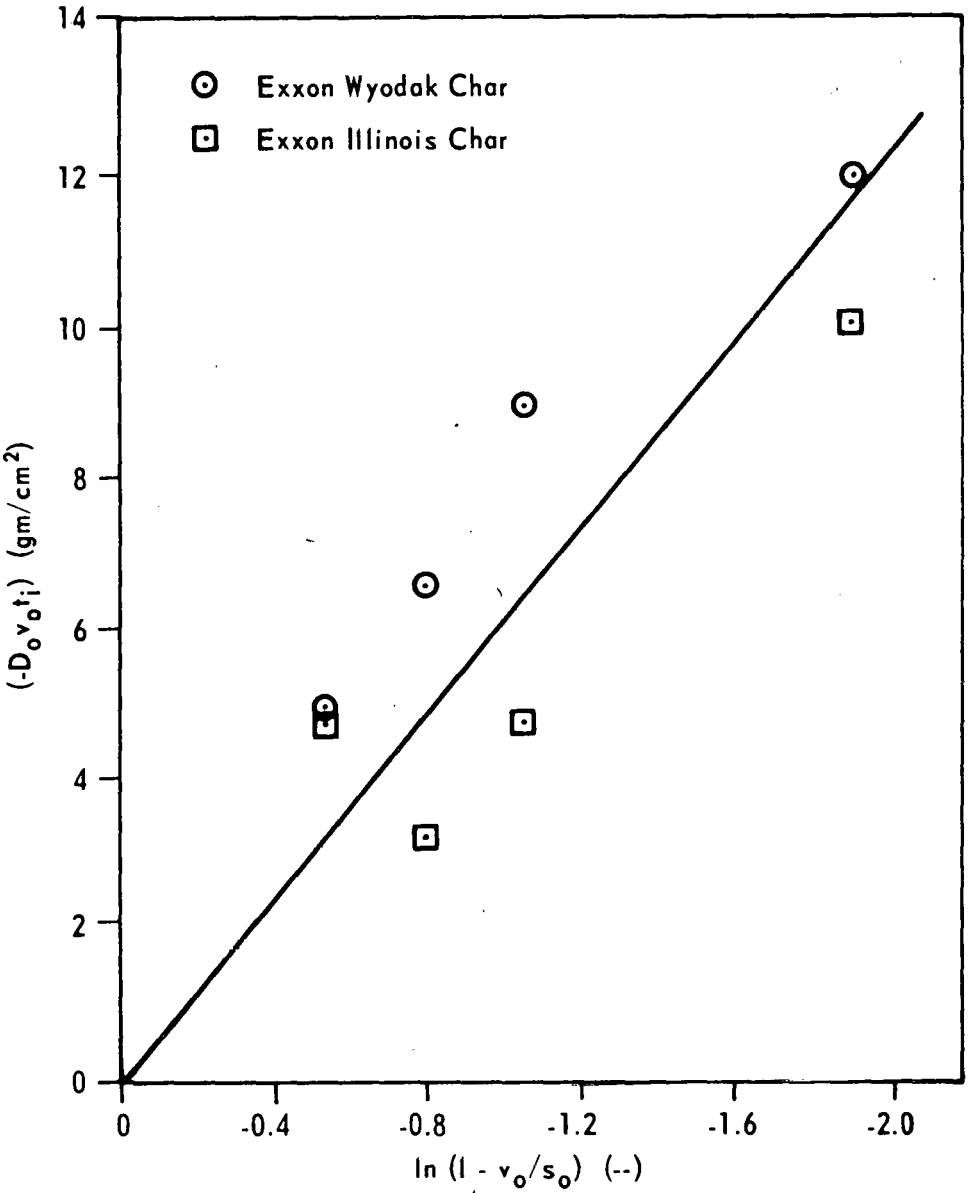

Figure 13 $(-D_0 v_0 t_i)$ VERSUS ln $(1 - v_0/s_0)$ FOR THE EXXON CHARS

Table 8. Variation of Ignition Distance with Fuel Type for 12.5 lb Fuel/hr at 8.8 scfm Air

Fuel	Ignition Distance (cm)	Ignition Time (sec)	S_o max (cm/sec)
Bituminous Coal	4		
E1 Char (Exxon)	5	0.089	42
E2 Char (Exxon)	5	0.086	42
B Char (BoM)	45	0.75	30
F Char (FMC)	50	1.07	18
Anthracite Ultra fine	40	0.79	17
Anthracite (UGI) regular grind	(unable to stabilize)		

For the inlet attenuation coefficient, a particle diameter of 25 μ with solid densities of 0.65 and 1.3 g/cc yielded values of 0.08 and 0.16 cm^{-1} (2.5 and 5.0 ft^{-1}) for k_o.

In addition, the reactivity was adjusted by use of the multiplicative favor, β. Values of β were taken from 0.11 to 1.0.

To match the most widely used experimental conditions, all calculations were carried out at 25 percent air deficiency. Consumption of all oxygen therefore corresponded to 75 percent burn-off (neglecting gasification which would only be important in the flame tail).

The calculation outputs included gas temperatures profiles with distance, maximum temperatures, and z-locations of maximum temperature (z_{opt}), 1 percent burn-off, ($z_{1\%}$) and 74 percent burn-off ($z_{74\%}$) (complete oxygen consumption). Flame thickness was arbitrarily defined as Δz_{1-74}.

The principal calculation objective was to show that flame position was significantly influenced by reactivity. The results selected for the purposes of this paper are summarized in Figures 14 and 15, and in Table 9.

Figure 14 illustrates both the general shape of the gas temperature profiles and the influence of reactivity by adjustment of the reactivity parameter, β. The coal/anthracite density of 1.3 g/cc was used in these calculations.

The nature of the computer program does not formally define ignition. A figure of 1 percent burn-off was therefore arbitrarily adopted as a close index of flame front location. This is indicated by the dashed line in Figure 14. It can be seen to occur at about 1000°C, which is about the experimental level reported by Howard and Essenhigh.[10-13] This temperature also rises somewhat with falling reactivity.

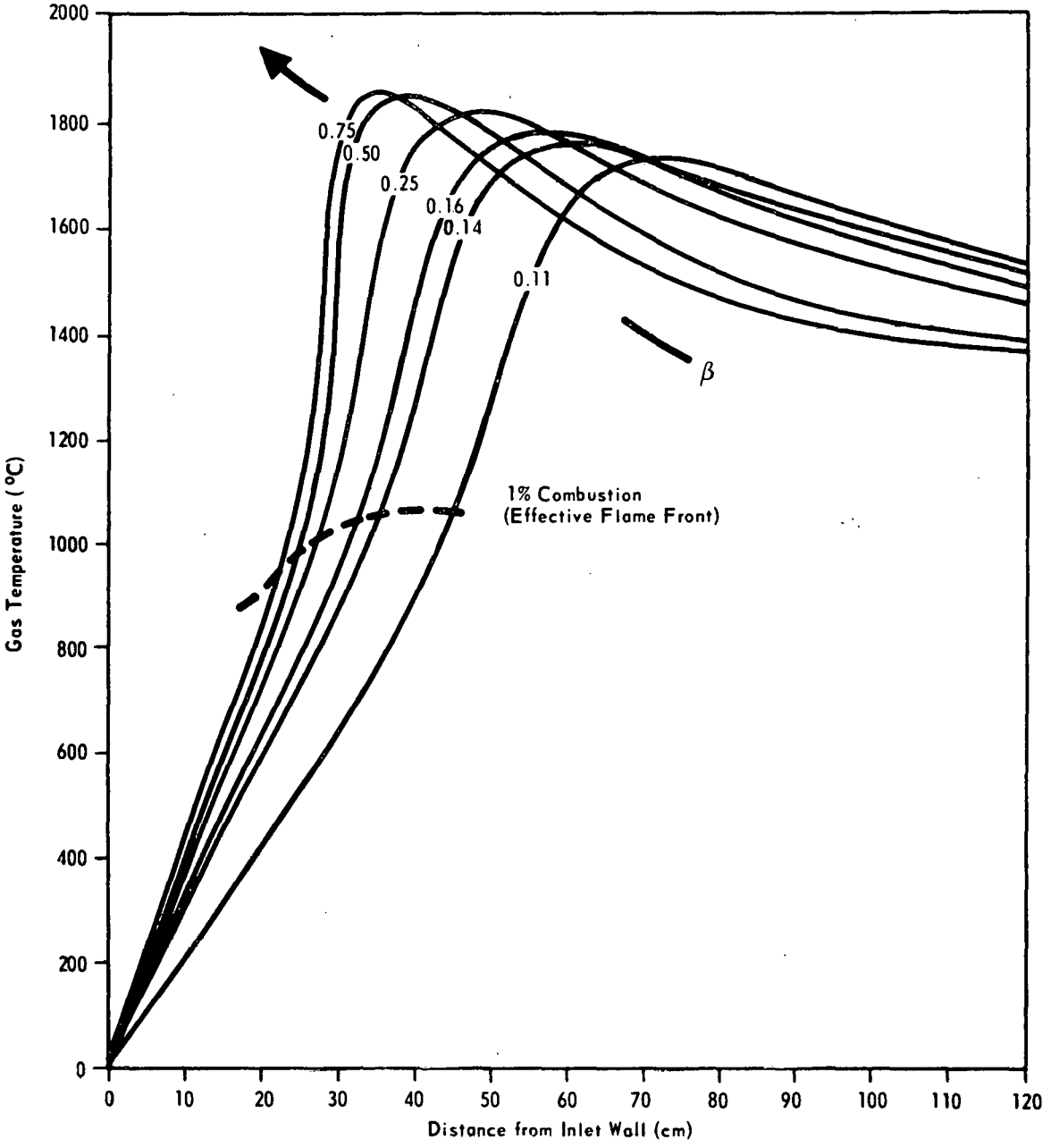

Figure 14 GAS TEMPERATURE VERSUS DISTANCE FOR k_0 = 0.08 cm^{-1} AND ρ_f = 0.65 gm/cc WITH β VARYING FROM 0.11 TO 0.75

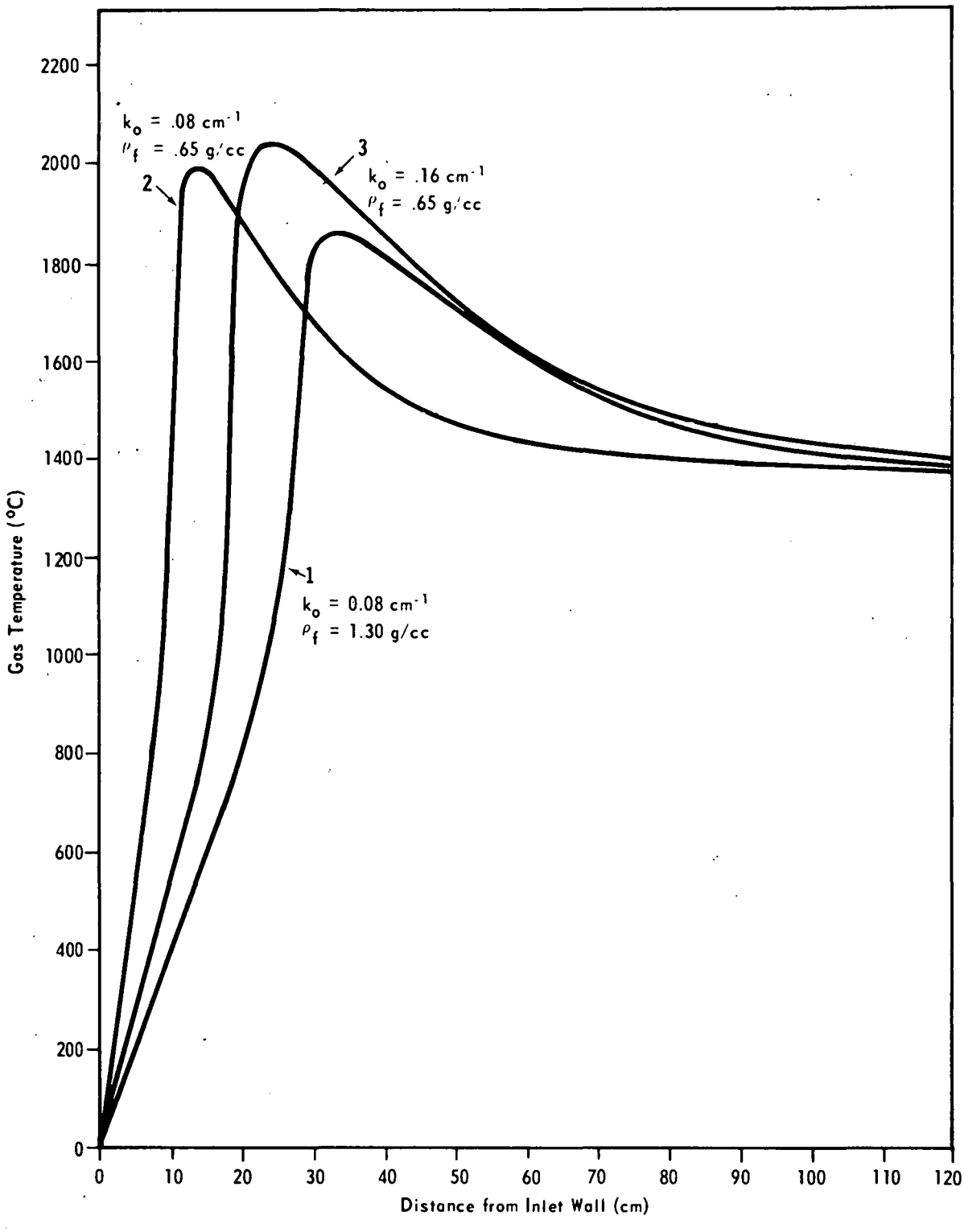

Figure 15 GAS TEMPERATURE VERSUS DISTANCE FOR VARIOUS VALUES OF k_o AND ρ_f

Table 9. Calculated Flame Positions and Associated Parameters

$k_o(cm^{-1})$	$\rho_f(g/cc)$	β	η_c	$T_{max}(°C)$	$z_{opt}(cm)$	$z_{1\%}(cm)$	$z_{74\%}(cm)$	$z_{1-74}(cm)$	$T_{w2}°C$	$T_{exit}°C$	$t_i(sec)$
0.16	0.65	0.75	75.00	1998	14.2	8.4	18.8	10.4	1338	1366	0.10
0.08	0.65	0.75	75.00	2048	23.5	16.8	27.0	10.2	1316	1388	0.22
0.08	1.3	0.75	75.00	1850	35.2	23.4	46.4	23.0	1261	1341	0.30
0.08	1.3	0.50	75.00	1853	38.4	24.6	56.0	31.4	1296	1378	0.32
0.08	1.3	0.25	74.77	1815	46.6	28.4	>120	--	1346	1441	0.36
0.08	1.3	0.16	73.70	1772	56.0	32.0	>120	--	1371	1489	0.41
0.08	1.3	0.14	72.95	1755	59.0	34.5	>120	--	1376	1505	0.44
0.08	1.3	0.11	70.09	1717	72.0	44.1	>120	--	1370	1536	0.56

Most significantly, however, the ignition distances indicated by this means are in the range roughly 20 to 50 cm which corresponds to the low reactivity group of ignition distances. The temperature peaks likewise move significant distances downstream with falling β, also by a factor of about 2.

The effect of changing from high density (1.3 g/cc) to low density (0.65 g/cm) is illustrated in Figure 15. Curve 1 of Figure 15 is included for comparison representing the curve for $\beta = 0.75$ on Figure 14 (at the high density). If the fuel density is halved at the same particle size, the particle density in the cloud is doubled, which doubles k_o. Curve 2 represents this condition, showing a significant increase in heating rate and roughly halving the ignition distance (1% burn-off point).

Curve 3 on Figure 15 is added to show the sensitivity to an arbitrary adjustment of the attenuation coefficient. Since halving the density doubles k_o from 0.08 to 0.16 cm^{-1}, the conditions for Curve 2 were re-examined at the original k_o value of 0.08 cm^{-1}. As can be seen, the flame temperature profile moves downstream yielding Curve 3, but not back to the original position of Curve 1. This clearly shows that fuel density is of comparable influence to the attenuation coefficient when k_o is adjusted independently of fuel density or vice versa. The flame "front", arbitrarily determined as before as the 1 percent burn-off point, shows comparable sensitivity to k_o and ρ_f. Again this point is observed at about 1000°C.

Similar results to the above are obtained at other values of β. Reproduction of addition curves provides no additional information of significance.

Table 9 lists behavior of the other parameters read out from the computations, including the location of the peak temperature (z_{opt}) and the flame "thickness", Δz_{1-74}. The conditions for the curves quoted are also tabulated here.

All but one of the calculations were carried out for $k_o = 0.08$ cm^{-1}. The first two entries compare the effect of change of fuel density (ρ_f) from the high reactivity equivalent (0.65) to the low reactivity equivalent (1.3). Column 3 is the reactivity parameter, (β), set at 0.75 for the first three entries, yielding the curves of Figure 14. The curves of Figure 13 are based on the data entries of rows 3 to 8 of the table. The plotted curves (Figures 13 and 14) include the "flame front locations identified as the 1 percent combustion point ($z_{1\%}$ in column 7); the curves also exhibit the optimum location for the peak temperature (z_{opt} in column 6); and the peak temperatures themselves, T_{max} (column 5).

The additional data provided by Table 9 therefore includes: the combustion efficiency leaving the furnace (η_c, column 4); the 74 percent combustion point ($z_{74\%}$, column 8, noting that, at the air deficient level calculated for, "complete" combustion or terminal oxygen consumption is 75%); the flame thickness Δz_{1-74} (column 9); the temperatures of the exit wall and of the exhaust gas (columns 10 and 11); and ignition time t_i (to $z_{1\%}$) (column 12).

The notable behavior here is the flame thickness. As the table shows, this is quite short (10 cm) for the low reactivity equivalent density, at a

value that is an order of magnitude shorter than found experimentally. The flame lengthens slowly and then dramatically as the reactivity is reduced.

In other results: (1) At $\beta = 0.75$, and the density is also kept constant, the flame thickness remains unchanged, but the ignition distance doubles as the attenuation coefficient is halved. (2) At constant k_o and β, doubling the fuel density slightly more than doubles the flame length, but the ignition distance also increases substantially, by about 50 percent. (3) Progressive reduction of the reactivity factor (β) at constant k_o and fuel density then shows the flame front moving steadily downstream with increase in flame length already noted. (4) Peak flame temperatures are on the high side, being approximately adiabatic for the fastest burning flames, and being still 100 to 150°C above experimental values for the slower burning flames. (5) The exit wall temperatures (T_{w2}) are an artifact of the model, being introduced both to model the furnace exit and as a cut-off to save computing time, but also shown (as described above) to be only weakly coupled to the upstream flame behavior. The flames are long enough that this does not significantly influence the combustion results.

It is evident that the simple radiation analysis[9] is adequate for high reactivity fuels where the ignition distance is a few centimeters, but with low reactivity fuels, a more elaborate analysis is necessary. The more elaborate analysis, presented in this paper, yields the projected result that ignition distance is then dependent on reactivity. There are further problems yet to be solved centering now on a more complete set of kinetic assumptions. It will also be of interest to develop the theoretical basis for defining ignition and applying it to this system. It would appear, nonetheless, that the theoretical description provided here is now broadly correct.

COMBUSTION OF COAL-OIL EMULSIONS

Introduction

Coal in amounts of up to 14 percent have been added to oil-water-air emulsions to determine heat transfer and combustion characteristics. The furnace efficiency peaked at about 5 percent coal addition at 10 percent water and 20 percent excess air. This behavior is attributed to a complex balance between the heat received by the load (water tubes on the furnace floor) directly from the flame and that received by the roof and walls but attenuated by transmission through the flame. Gas exit temperatures fell as efficiency rose at constant excess air (coal addition), and vice versa, substantiating this argument.

Experimental

In previously reported studies of oil-water-air (MGD) emulsions,[15] the thermal efficiency of hot wall furnace with water tubes on the furnace floor was found to fall with increasing water content in the emulsion. The effect was attributed to change of flame emissivity since exit gas temperatures rose. Addition of particles at very low loading restored the heat transfer, as already reported.[15] Extension of those particle addition studies to higher concentrations has now shown that the efficiency improvement peaks and then declines again. In a first sequence of experiments using the original can-type burner, particles were supplied to the flame by operating beyond the smoke point (from +10% to -5% excess air). Even at 90 percent smoke, particulate measurements showed less than 1 percent combustible loss so the effective thermal input hardly changed. In a second sequence of experiments, using a commercial (York-Shipley), air-atomizing burner, coal was added to the emulsion, with adjustment of the oil rate in this instance to maintain the thermal input at about 1.25 million Btu/hr and excess air constant. Efficiency peaked at about 50 percent smoke at all water levels up to 37.5 percent (Figure 16). Efficiency peaked at about 5 percent in the coal/oil dispersion at 10 percent water and 20 percent excess air (Figure 17).

The behavior is attributed to a complex balance between heat received by the load (water tubes on the furance floor) directly from the flame and that received from the roof and walls, but attenuated by transmission through the flame. With a low emissivity flame, two thirds or more of the heat picked up by the load comes from the roof and walls. As flame emissivity (absorptivity) rises, there is more direct heat transfer from the flame, but more of the roof and wall radiation is absorbed by the flame gases. Initially, the flame contribution increases with a less-than-corresponding decrease in the roof and wall contribution, and the net rises. At high emissivities, the reverse is the case, and the net falls. The result is the efficiency peaking observed (Figure 18). Further substantiating this interpretation, gas exit temperatures fell as efficiency rose at constant excess air (coal addition) and vice versa (Figure 18). In the smoke experiments interpretation is more complex since there is improved efficiency due to reduced excess air. This, however, only accounts for about half the efficiency increase. Moreover, gas exit temperatures were broadly unchanged whereas they would have increased had the efficiency improvement been due to reduced excess air alone.

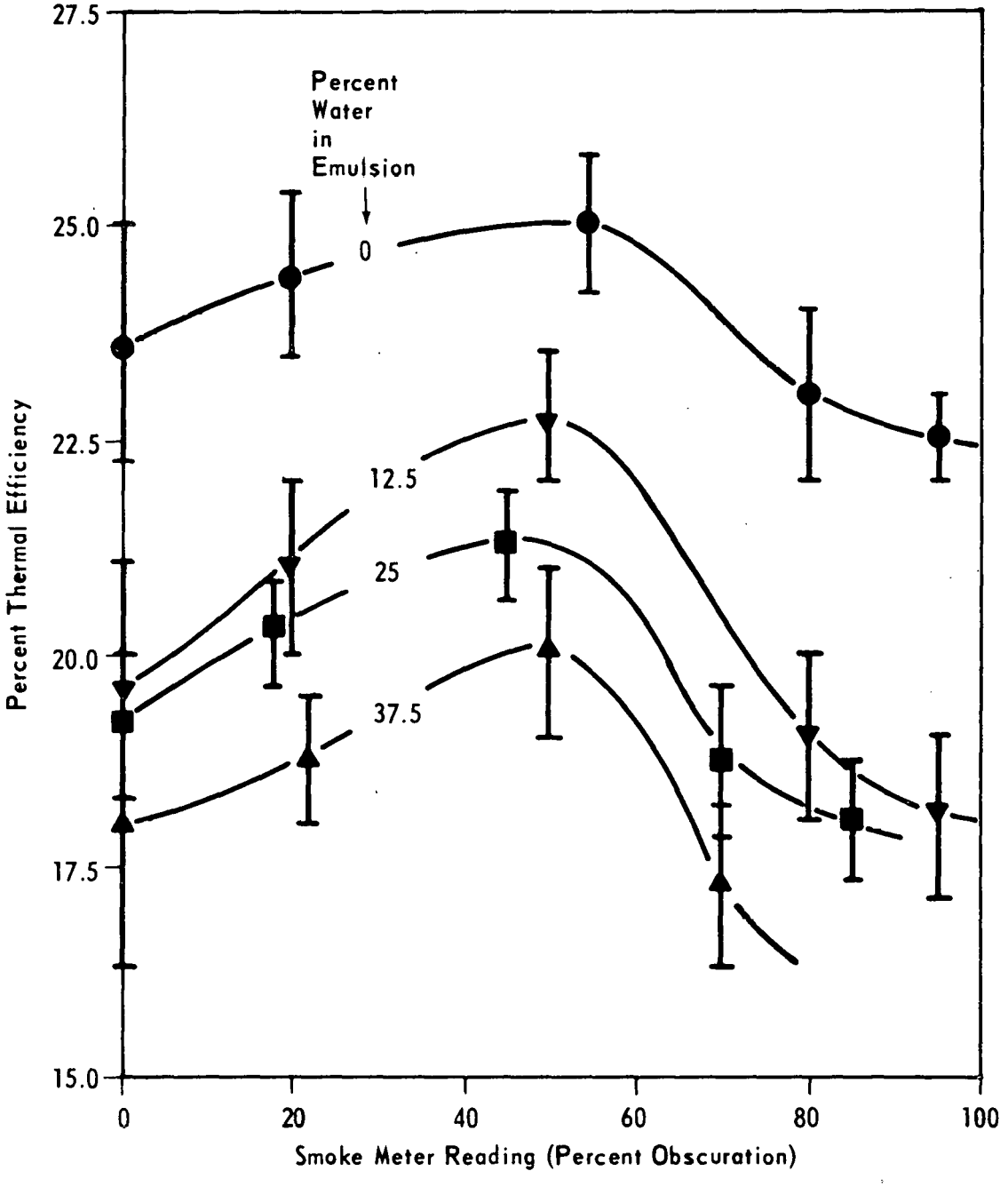

Figure 16 VARIATION OF THE OVERALL THERMAL EFFICIENCY OF THE FURNACE AS A FUNCTION OF SMOKE METER READING (PERCENT OBSCURATION) FOR DIFFERENT LEVELS OF WATER ADDITION (BARS DENOTE STANDARD ERROR)

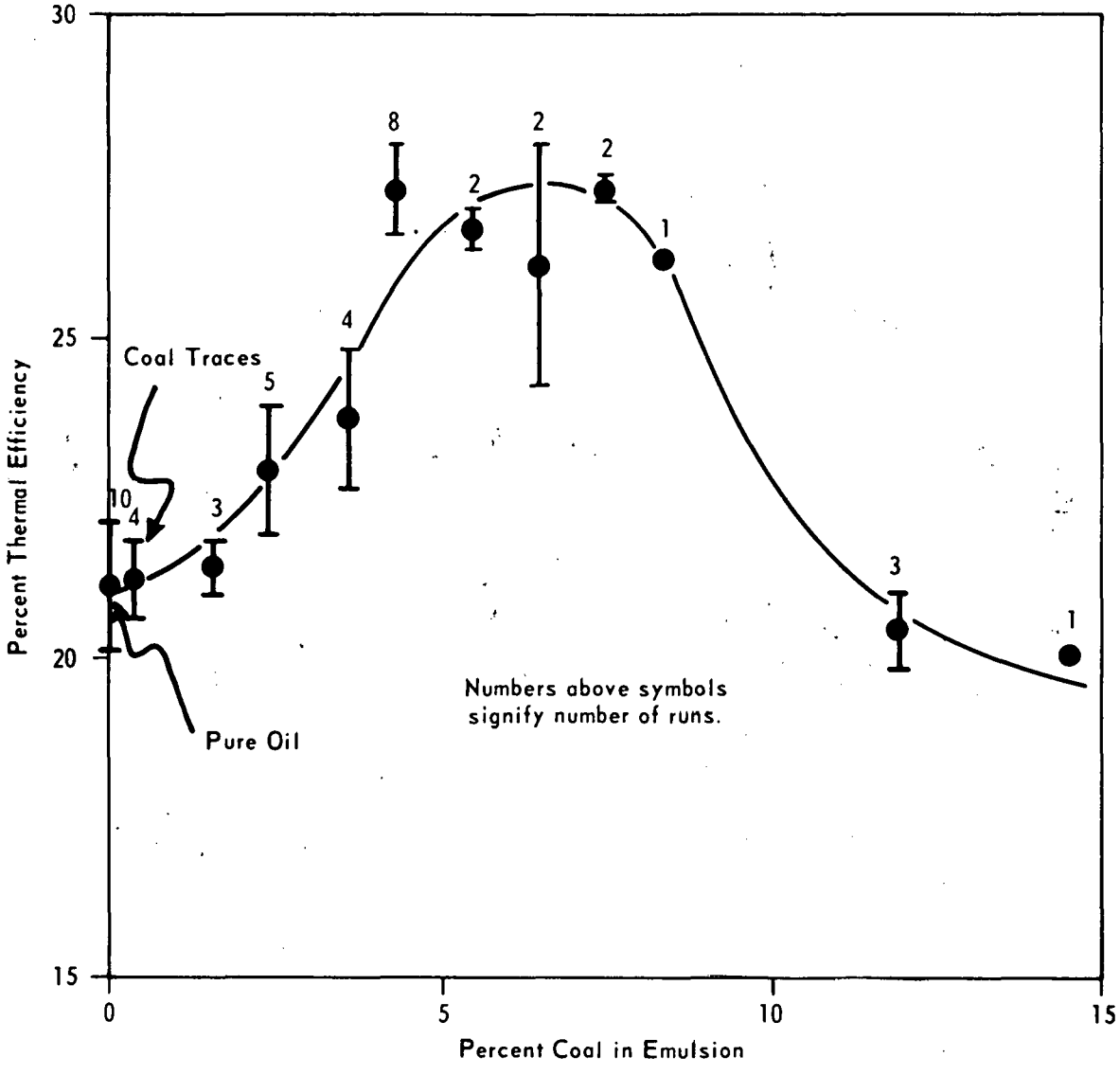

Figure 17 VARIATION OF THE OVERALL THERMAL EFFICIENCY OF THE FURNACE AS A FUNCTION OF COAL PERCENTAGE ADDED TO COAL/OIL DISPERSION AT 10 PERCENT WATER WITH 20 PERCENT EXCESS AIR

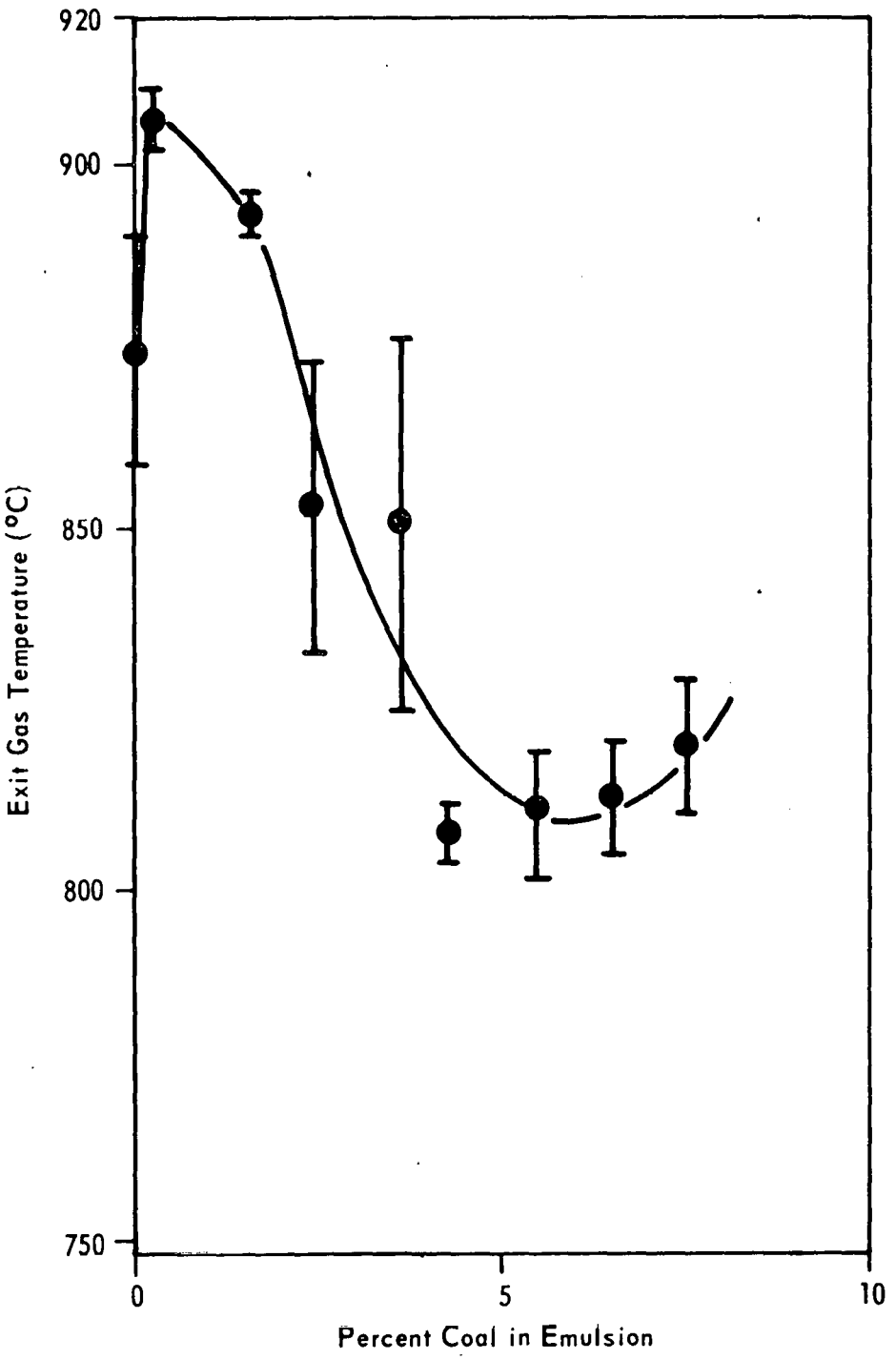

Figure 18 VARIATION OF THE GAS EXIT TEMPERATURE AS A FUNCTION OF THE COAL PERCENTAGE ADDED (BARS DENOTE STANDARD ERROR)

CONCLUSIONS

1. A cold model study of the air flow through a packed bed has shown the pressure drop through the bed to be directly proportional to the square of the velocity, consistent with results reported previously. In addition, the pressure drop was found to be inversely proportional to the square of the mean particle diameter.

2. Results of theoretical calculations indicate that chemical, kinetic, physical, and geometric parameters considered simultaneously can have a significant effect on the thermal history of a coal particle under pyrolysis conditions.

3. The mass spectrometer and reactor systems can be used to measure the amount of vaporization (and pyrolysis) products of hydrocarbons in low concentrations in a helium carrier gas.

4. Negative values of weight loss and burnoff were observed in the early stages of pyrolysis and combustion of PSOC-246 originally size graded to 270 x 400 mesh. These values resulted from a net loss in ash contents of the corresponding chars compared to the ash content of the parent coal. The statistical meaning of these results is under investigation. The total burnoff of the PSOC-246 size grade studied in air approaches 80 percent (daf basis) in 300 msec, whereas weight loss due to pyrolysis in nitrogen is only slightly above 21 percent (daf basis). The contrast in these figures should be reflected in the physical characteristics of their corresponding chars.

5. Water densities of seventeen coals of different rank have been determined at 25°C. These densities show 'drift' with time but attain constant limiting values after five days. Water densities are invariably higher than the helium densities. This behavior is different from that reported in the literature.

6. Small angle x-ray scattering has proved to be a valuable tool for characterizing the pore structure of coal chars. It has been shown that the pore structure of a char is a function of the rank of the parent coal and the maximum heat treatment temperature.

7. Carbon deposition decreases subsequent reactivity of char to air. The decrease in reactivity appears to be due to a decrease in active surface area and deactivation of catalytic impurities. Deposited carbon is much less reactive to air than is the lignite char. The results indicate that in order to maximize subsequent char reactivity to oxidizing gases, carbon deposition from volatiles during the conversion of coal to char should be kept to a minimum.

8. For the oxygen activated Saran carbon (activated to 63.8% carbon burnoff) the total 'active' area, (determined mass-spectrometrically) accessible to oxygen during chemisorption of 100°C, is 26.0 m^2/g carbon. This represents only 3.05 percent of the total area determined from carbon dioxide adsorption at 298°K. Increase in soak time at 600°C prior to

chemisorption at 100°C decreases both Q (cal/g carbon) and W (mg oxygen/g carbon). However, ΔH (kcal/mole oxygen chemisorbed) is essentially independent of soak time. ΔH in the surface coverage region 0.675 - 0.746 is 70.5 ± 1.3 kcal/mole.

9. Siderite, calcite, and gypsum catalyze the cracking of methane. The products of the reaction have been identified by x-ray diffraction studies. Siderite gives iron and highly crystalline carbon; the deposited carbon had an interlayer spacing of 3.371 Å and an average crystallite height of 500 Å. A very broad (002) diffraction peak was found for carbon deposited over calcium oxide (derived from calcite) indicating that the carbon formed had a very small crystallite size. Gypsum reacted with methane giving calcium sulfate (anhydrite), calcium oxide, and calcium sulfide although no surface deposition of carbon was observed.

10. Combustion research on chars and low volatile fuels indicates that low volatile content does not necessarily imply low reactivity in the case of man-made fuels, unlike naturally occurring fuels such as anthracites. Internal pore structure does determine resultant reactivity. Reactivity is controlled by the particular coal conversion process used to produce the char rather than the parent coal. Particle size can be increasingly important for fuels of low reactivity as any internal surface becomes decreasingly accessible. Ignition distance was found to be approximately proportional to inlet velocity, yielding approximately constant ignition times, for small t_i. For t_i not small, the relation between L_i and t_i becomes non-linear.

11. Ignition times for the high reactivity fuels were found in good agreement with established simple radiation theory, but the ignition times for the low reactivity fuel are substantially greater than the predictions of this same theory, and agreement with theory is questionable. No evidence for particle shattering and/or swelling in the pre-ignition region was found, thus eliminating it as a reason for the variation in behavior between the low and high reactivity fuels. Radiation from the bottom of the furnace, that could have been an artificial stabilizer for the low reactivity flames, was found to have only second order effects at best, and could be disregarded. The only aspect of behavior not satisfactorily explained in principle in the results and analysis so far presented is the order of magnitude difference in ignition times between the high and low reactivity fuels. The discrepancy is being accounted for in a more elaborate radiation model.

12. Coal in amounts up to 14 percent have been added to oil-water-air emulsions to determine heat transfer and combustion characteristics. The furnace efficiency peaked at about 5 percent coal addition at 10 percent water and 20 percent excess air. This behavior is attributed to a complex balance between the heat received by the load (water tubes on the furnace floor) directly from the flame and that received by the roof and walls but attenuated by transmission through the flame. Gas exit temperatures fell as efficiency rose at constant excess air (coal addition), and vice versa, substantiating this argument.

REFERENCES

1. Eapen, T., R. Blackadar, and R.H. Essenhigh. Sixteenth International Symposium on Combustion, Pittsburgh, Pennsylvania, 1976 (in press).

2. Spackman, W., A. Davis, P.L. Walker, H.L. Lovell, R.H. Essenhigh, F.J. Vastola, and P.H. Given. The Characteristics of American Coals in Relation to Their Conversion into Clean Energy Fuels. Qtr. Tech. Prog. Rept. FE-2030-6 of The Pennsylvania State University to ERDA, 61 pp., March, 1977.

3. Nsakala, N. The Characteristics of Chars Produced by Pyrolysis Following Rapid Heating of Pulverized Coal. Doctoral Thesis of The Pennsylvania State University. 201 pp., 1976.

4. Field, M.A., D.W. Gill, B.B. Morgan, and P.G.W. Hawksley. Combustion of Pulverized Coal. BCURA, Leatherhead, England, p. 250, 1967.

5. Kobayashi, H., J.B. Howard, and A.F. Sarofim. Sixteenth International Symposium on Combustion, Pittsburgh, Pennsylvania, 1976 (in press).

6. Tschamber, H., and E. de Ruiter. Physical Properties of Coals, in Chemistry of Utilization, H.H. Lowry (ed.), John Wiley, New York, Suppl. vol., p. 35, 1963.

7. Ettinger, I.L., and E. Zhupakhina. Method of Determining Porosity of Mineral Coals. Fuel, vol. 39, p. 387, 1967.

8. Spackman, W., A. Davis, P.L. Walker, H.L. Lovell, R.H. Essenhigh, F.J. Vastola, and P.H. Given. The Characteristics of American Coals in Relation to Their Conversion into Clean Energy Fuels. Qtr. Tech. Prog. Rept. FE-2030-3 of The Pennsylvania State University to ERDA, 185 pp., May, 1976.

9. Essenhigh, R.H., and J. Csaba. Ninth International Symposium on Combustion, Academic Press, New York, p. 111, 1963.

10. Howard, J.B., and R.H. Essenhigh. Combustion and Flame, vol. 9, p. 337, 1965.

11. _____. Combustion and Flame, vol. 10, p. 92, 1966.

12. _____. Ind. Eng. Chem. Proc. Res. & Dev., vol. 6, p. 74, 1967.

13. _____. Eleventh International Symposium on Combustion, The Combustion Institute, Pittsburgh, p. 399, 1967.

14. Essenhigh, R.H., and J.G. Cogoli. Pulverized Char Combustion in a Laboratory Scale Furnace. 170th National Meeting ACS, Div. of Fuel Chemistry, vol. 20, no. 3, p. 134, 1975.

15. Essenhigh, R.H., A. Kokkinos, and others. Smoke Point and Heat Transfer Characteristics of Oil/Water/Air Emulsions Without and With Coal Addition in a Hot Wall Furnace. Central States Section, Combustion Institute, Batelle Memorial Institute, April, 1976.

16. Krisinger, H., F.K. Ovitz, and C.E. Hugustine. U.S. Bureau of Mines, Technical Paper No. 137, 1916.

The following individuals have made contributions to this report: J.C. Cogoli, C.P. Dolsen, T. Eapen, J. Friehaut, H. Gong, E. Gootzait, D.S. Hoover, J.M. Hower, I.K. Ismail, R.G. Jenkins, M. Kamishita, A. Kokkinos, K.W. Kuehn, A.A. Leff, A. Linares, O.P. Mahajan, N. Nsakala, F.M. Seagaard, H.E. Shull, N.H. Suhr, and A. Youssef.

☆U.S. GOVERNMENT PRINTING OFFICE: 1978-740-206/116